

# Astrophysical Objects

## Active Galaxies

Based on: An introduction to modern Astrophysics chapter 28

**Helga Dénés 2023 S2 Yachay Tech**  
[hdenes@yachaytech.edu.ec](mailto:hdenes@yachaytech.edu.ec)



**SCHOOL OF  
PHYSICAL SCIENCES  
AND NANOTECHNOLOGY**

# Gravitational lensing

Quasars are among the most distant visible objects in the universe, and so they offer a unique opportunity to probe the intervening space. Clouds of gas, galaxies, and dark matter can all affect the light from a quasar during its journey to Earth. By decoding the clues supplied by observations of quasars, astronomers can learn a great deal about the perturbing objects along the line of sight.

In 1919, the same year that Eddington measured the bending of starlight as it passed near the Sun and verified Einstein's general theory of relativity, Sir Oliver Lodge (1851–1940), an English physicist, put forth the possibility of **using a gravitational lens to focus starlight**. During the 1920s, astronomers began to consider how **light passing through the curved spacetime surrounding a massive object could produce multiple images of the source**.

Then, in 1937, Fritz Zwicky (1898–1974) proposed that **gravitational lensing by a galaxy** would be much more likely than gravitational lensing by individual stars.

# Gravitational lensing

By the 1970s the search was on for a multiply imaged quasar, and in 1979 the quasar Q0957+561 was discovered to appear twice in the sky. As shown in Fig. 33, the two images are separated by  $6.15''$ , and each shows a **quasar with a redshift of  $z = 1.41$ .**

The **gravitational lens** is due to the gravity of an **intervening giant galaxy** with  $z = 0.36$  that is between the two images and  $0.8''$  away from one of them.

**How do we know that they are the same galaxy?**

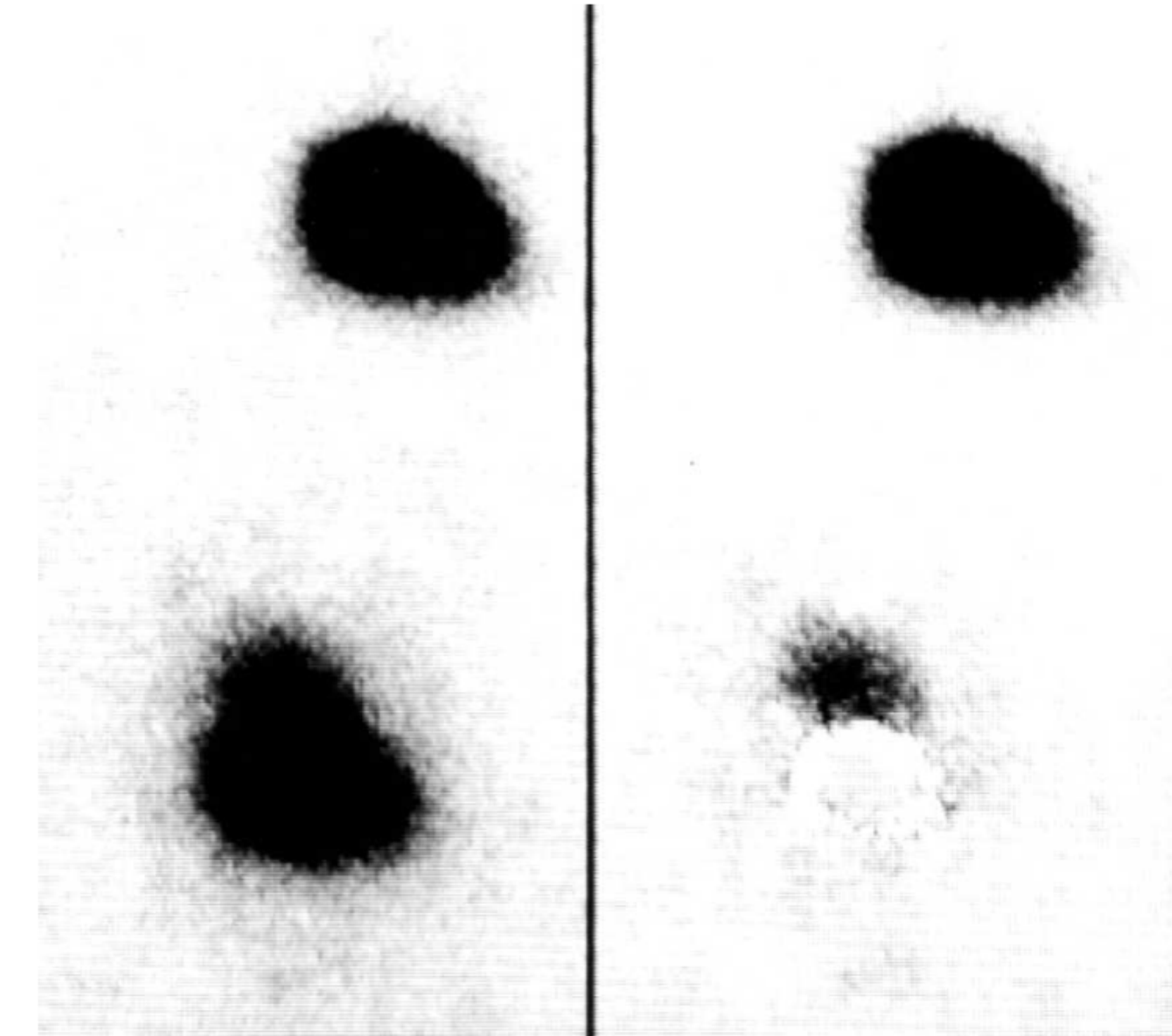


**FIGURE 33** An optical (negative) view of the double quasar Q0957+561. The photo on the left shows the two gravitationally lensed images. The fuzz extending upward from the bottom image is the lensing galaxy. On the right, the upper image has been subtracted from the lower image to reveal the lensing galaxy more clearly. (Figure from Stockton, *Ap. J. Lett.*, 242, L141, 1980.)

# Gravitational lensing

In addition to having the **same redshift**, both images have the **same two bright emission lines** and **many absorption features in common**. Both images also show the **same radio core and jet structure**.

Figure 34 shows **spectra** of the two images of **another quasar**, Q0142–100, that are also formed by a gravitational lens. Like optical lenses, **gravitational lenses can magnify and increase an object's brightness**.

(The difference in the apparent magnitudes of the images of Q0142–100 is about  $\Delta m_V = 2.12$ .)

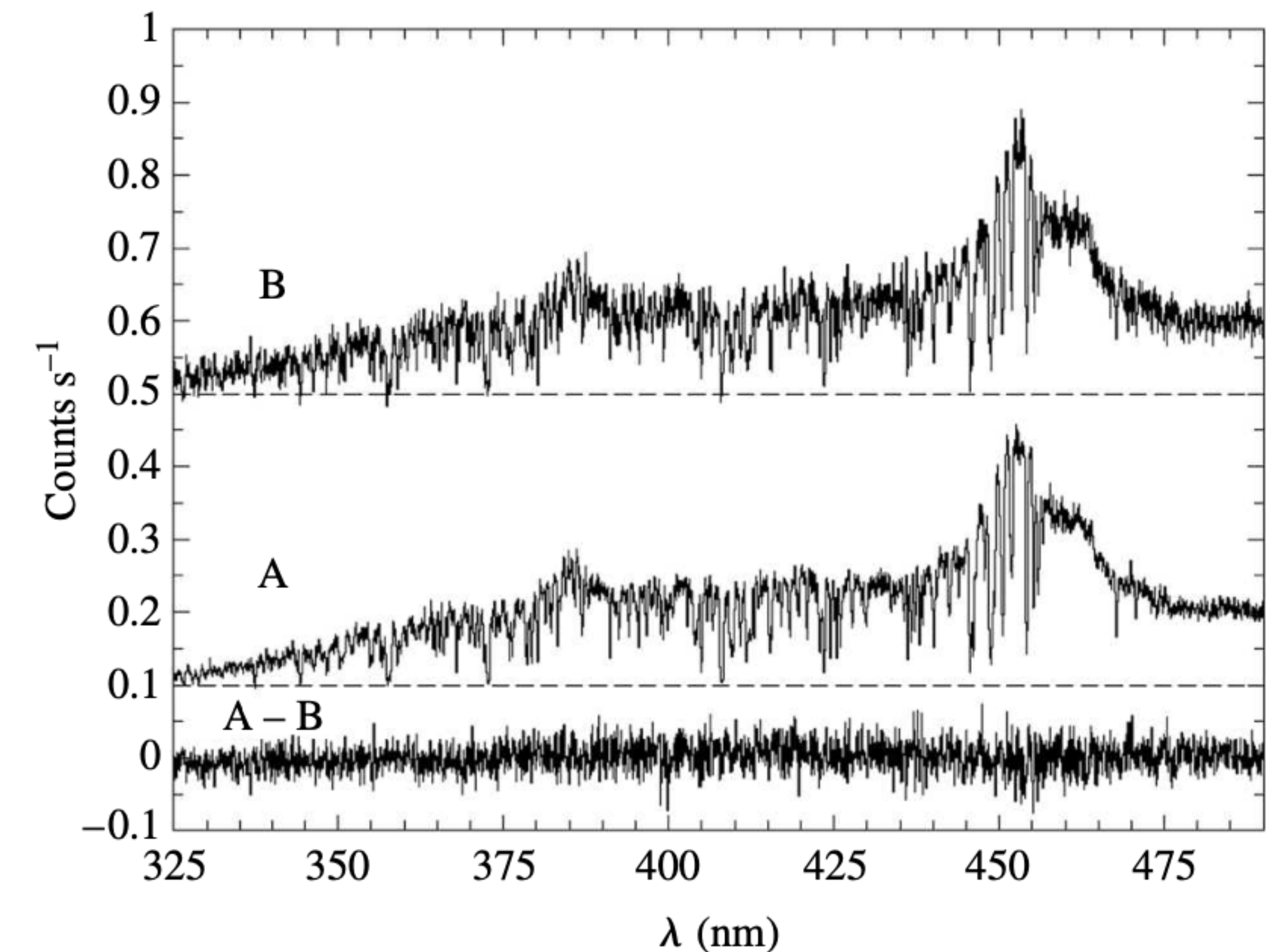


**FIGURE 34** Spectra of the images of the quasar Q0142–100 formed by a gravitational lens. The bottom panel shows the difference between the two spectra. (Figure adapted from Smette et al., *Ap. J.*, 389, 39, 1992.)

# The geometry of gravitational lensing

Gravitational lensing results when light follows the straightest possible worldline (a geodesic) as it travels through the curved spacetime around a massive object. It is analogous to the normal refraction of light by a glass lens that occurs as the light crosses the lens surface, passing from one index of refraction,  $n$ , to another, where  $n \equiv c/v$  is just the ratio of the speed of light in a vacuum to its speed,  $v$ , in the medium. Outside of a spherical object of mass  $M$  (which is equivalent to a point mass), the coordinate speed of light in the radial direction is given by,

$$\frac{dr}{dt} = c \left( 1 - \frac{2GM}{rc^2} \right)$$

so the effective “index of refraction” is

$$n = \frac{c}{dr/dt} = \left( 1 - \frac{2GM}{rc^2} \right)^{-1} \simeq 1 + \frac{2GM}{rc^2}$$

# The geometry of gravitational lensing

for radially traveling light, assuming that  $2GM/rc^2 \ll 1$ . At a distance of  $10^4$  pc from a galaxy with a mass of  $10^{11} M_\odot$ , the effective index of refraction is  $n = 1 + 9.6 \times 10^{-7}$ . (Of course, the light passing by the point mass will never be traveling exactly radially. This was merely used to estimate the magnitude of the effect of gravity in a gravitational lens.) Obviously, the deviation of the light from a straight line will be extremely small.

Figure 35 shows the **path taken by light** from a source at point S, as it is deflected through an angle,  $\phi$ , by the gravitational lens due to a point mass, M, at point L. The light arrives at the position of the observer at point O.

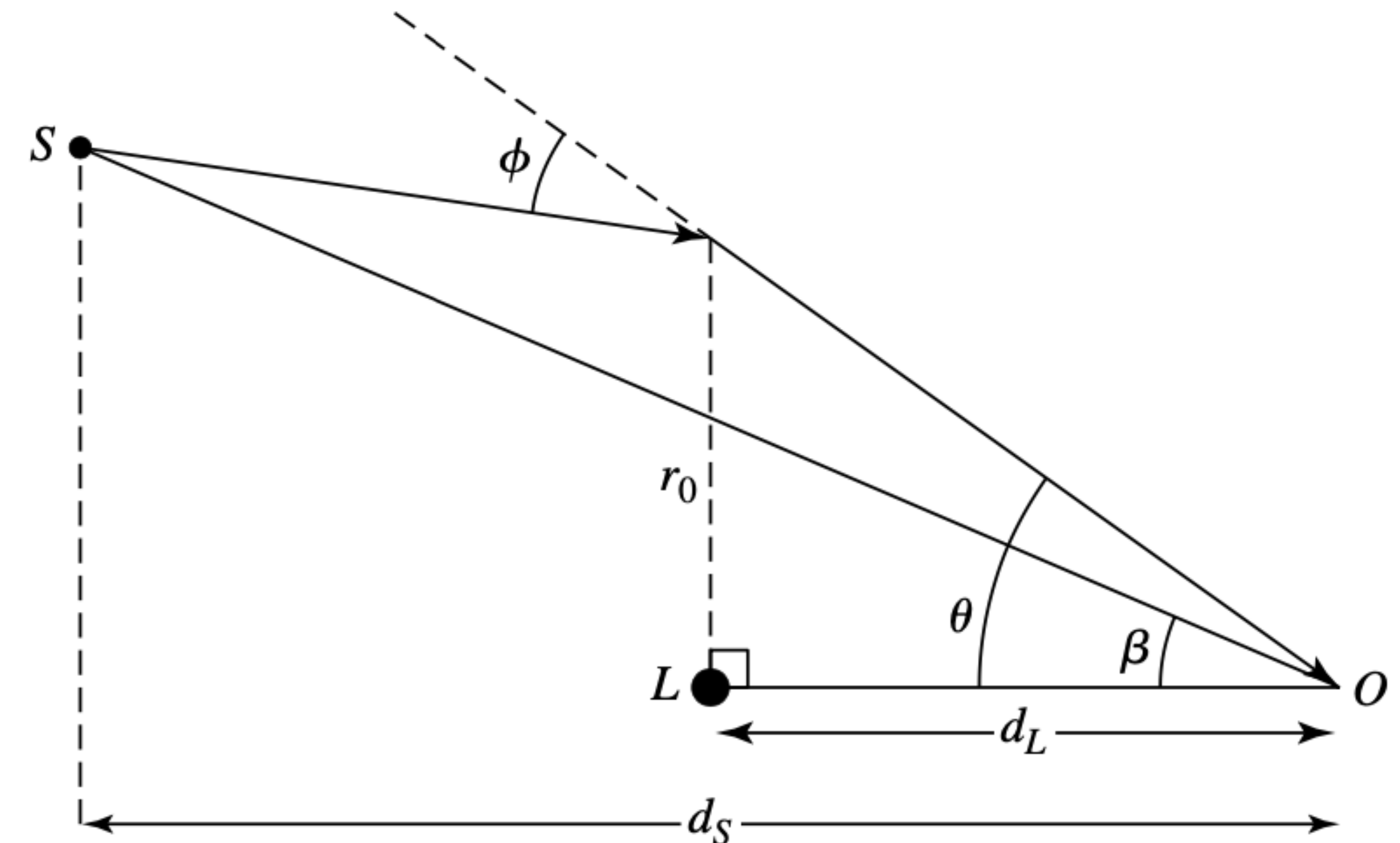


**FIGURE 35** The geometry for a gravitational lens. Light from the source, S, passes within a distance of approximately  $r_0$  of a lensing point mass at L on its way to an observer at O. The angles involved are actually just a fraction of a degree, and so  $r_0$  is very nearly the distance of closest approach.

# The geometry of gravitational lensing

The angular deviation of a photon passing a distance  $r_0$  from a mass  $M$  was

$$\phi = \frac{4GM}{r_0 c^2} \text{ rad}$$

The distance to the source is  $d_S / \cos \beta \approx d_S$ , where  $\beta \ll 1$ , and  $d_L$  is the distance to the lensing mass. It is then a matter of simple trigonometry to show that the **angle  $\theta$  between the lensing mass and the image of the source** must satisfy the equation

$$\theta^2 - \beta\theta - \frac{4GM}{c^2} \left( \frac{d_S - d_L}{d_S d_L} \right) = 0,$$

where  $\theta$  and  $\beta$  are measured in radians.

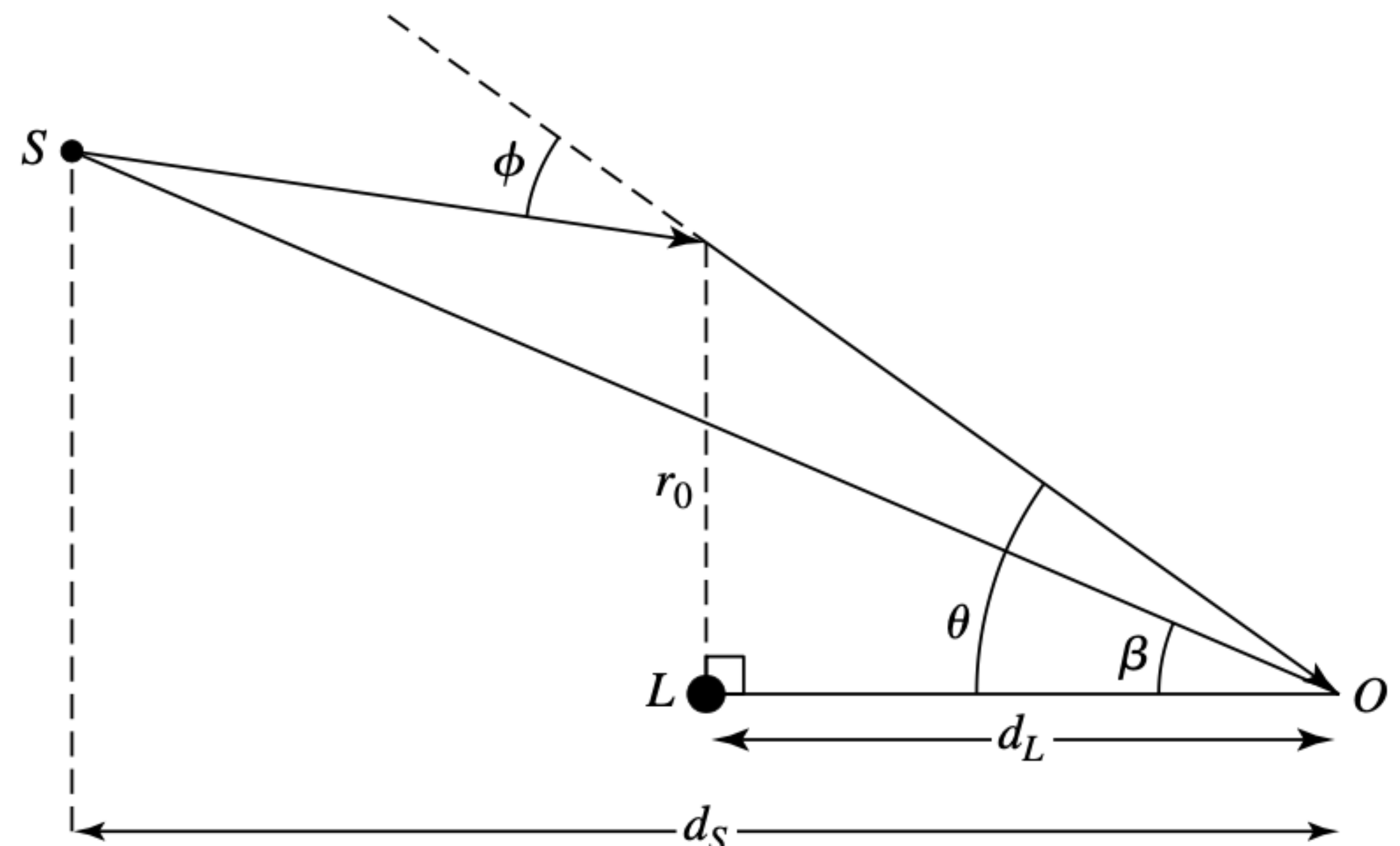


**FIGURE 35** The geometry for a gravitational lens. Light from the source,  $S$ , passes within a distance of approximately  $r_0$  of a lensing point mass at  $L$  on its way to an observer at  $O$ . The angles involved are actually just a fraction of a degree, and so  $r_0$  is very nearly the distance of closest approach.

# The geometry of gravitational lensing

The quadratic equation indicates that for the geometry shown in the figure, there will be two solutions for  $\theta$ , and so **two images will be formed by the gravitational lens**. Designating these solutions as  $\theta_1$  and  $\theta_2$ , these angles can be measured observationally and then used to find the values of  $\beta$  and  $M$ . The results are

$$\beta = \theta_1 + \theta_2.$$

$$M = -\frac{\theta_1 \theta_2 c^2}{4G} \left( \frac{d_S d_L}{d_S - d_L} \right).$$

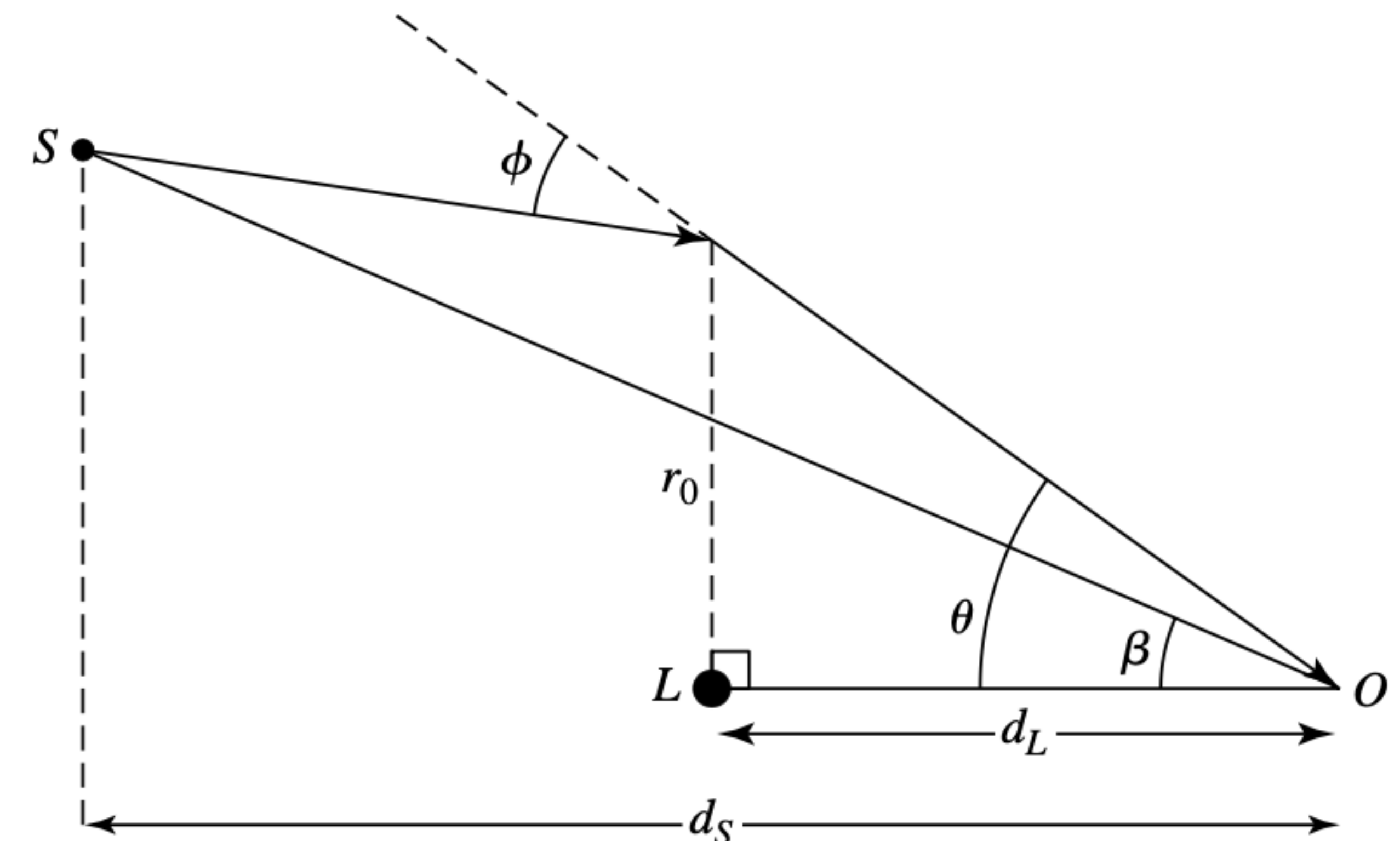


**FIGURE 35** The geometry for a gravitational lens. Light from the source,  $S$ , passes within a distance of approximately  $r_0$  of a lensing point mass at  $L$  on its way to an observer at  $O$ . The angles involved are actually just a fraction of a degree, and so  $r_0$  is very nearly the distance of closest approach.

# The geometry of gravitational lensing

Referring back to Fig. 35, note that **θ<sub>1</sub> and θ<sub>2</sub> have opposite signs**. As a result, the two images are formed on **opposite sides of the gravitational lens**, so M will be positive.

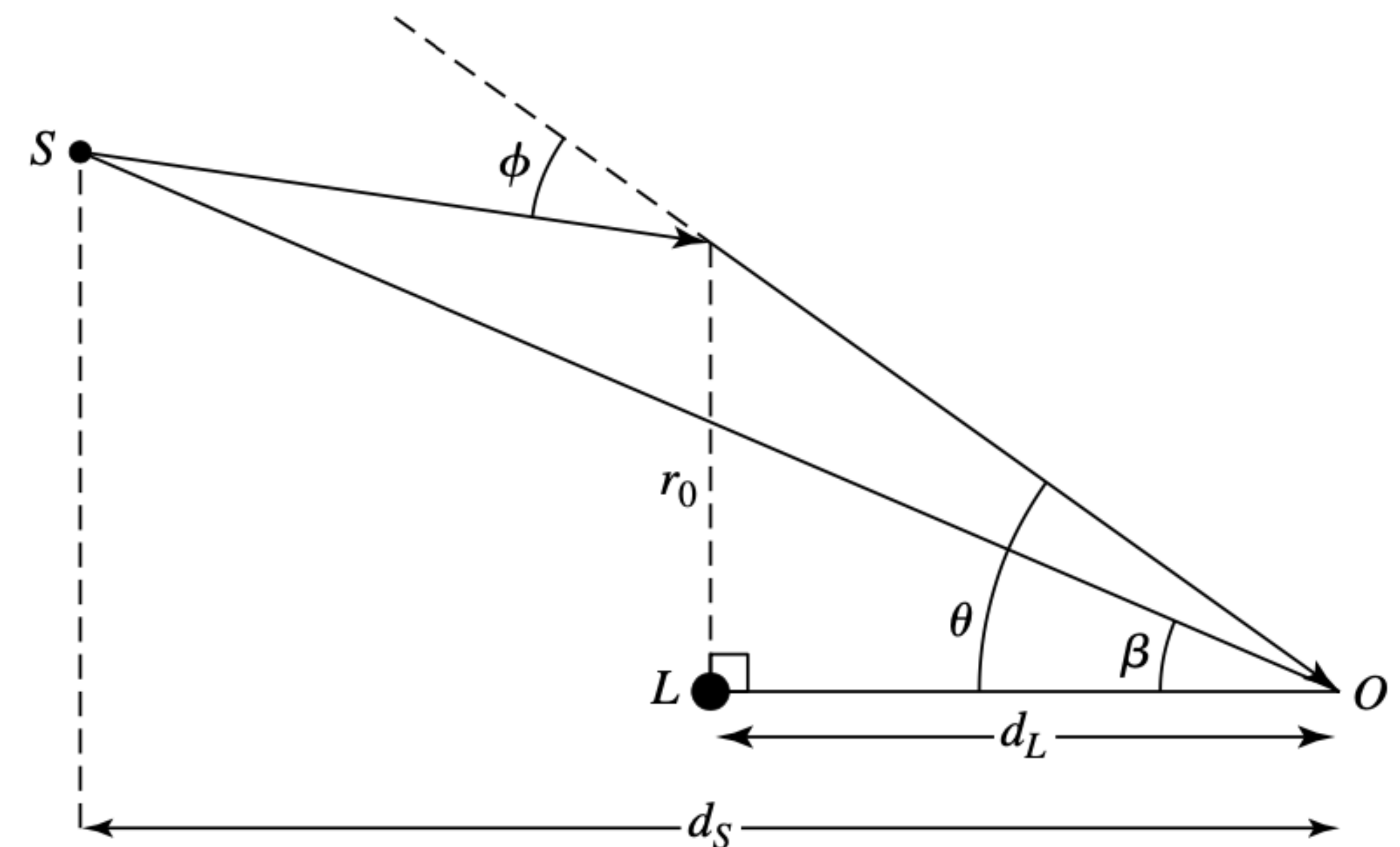


**FIGURE 35** The geometry for a gravitational lens. Light from the source,  $S$ , passes within a distance of approximately  $r_0$  of a lensing point mass at  $L$  on its way to an observer at  $O$ . The angles involved are actually just a fraction of a degree, and so  $r_0$  is very nearly the distance of closest approach.

# The geometry of gravitational lensing

**Example 4.1.** For the quasar Q0957+561 shown in Fig. 33,  $\theta_1 = 5.35'' = 2.59 \times 10^{-5}$  rad, and  $\theta_2 = -0.8'' = -3.88 \times 10^{-6}$  rad. (Which angle assumes the minus sign is arbitrary.) From the quasar's redshift of  $z_S = 1.41$  and the gravitational lens redshift of  $z_L = 0.36$ , the Hubble law gives the corresponding distances of  $d_S = 2120h^{-1}$  Mpc and  $d_L = 890h^{-1}$  Mpc. Then

$$M = -\frac{\theta_1 \theta_2 c^2}{4G} \left( \frac{d_S d_L}{d_S - d_L} \right) = 8.1 \times 10^{11} h^{-1} M_\odot.$$

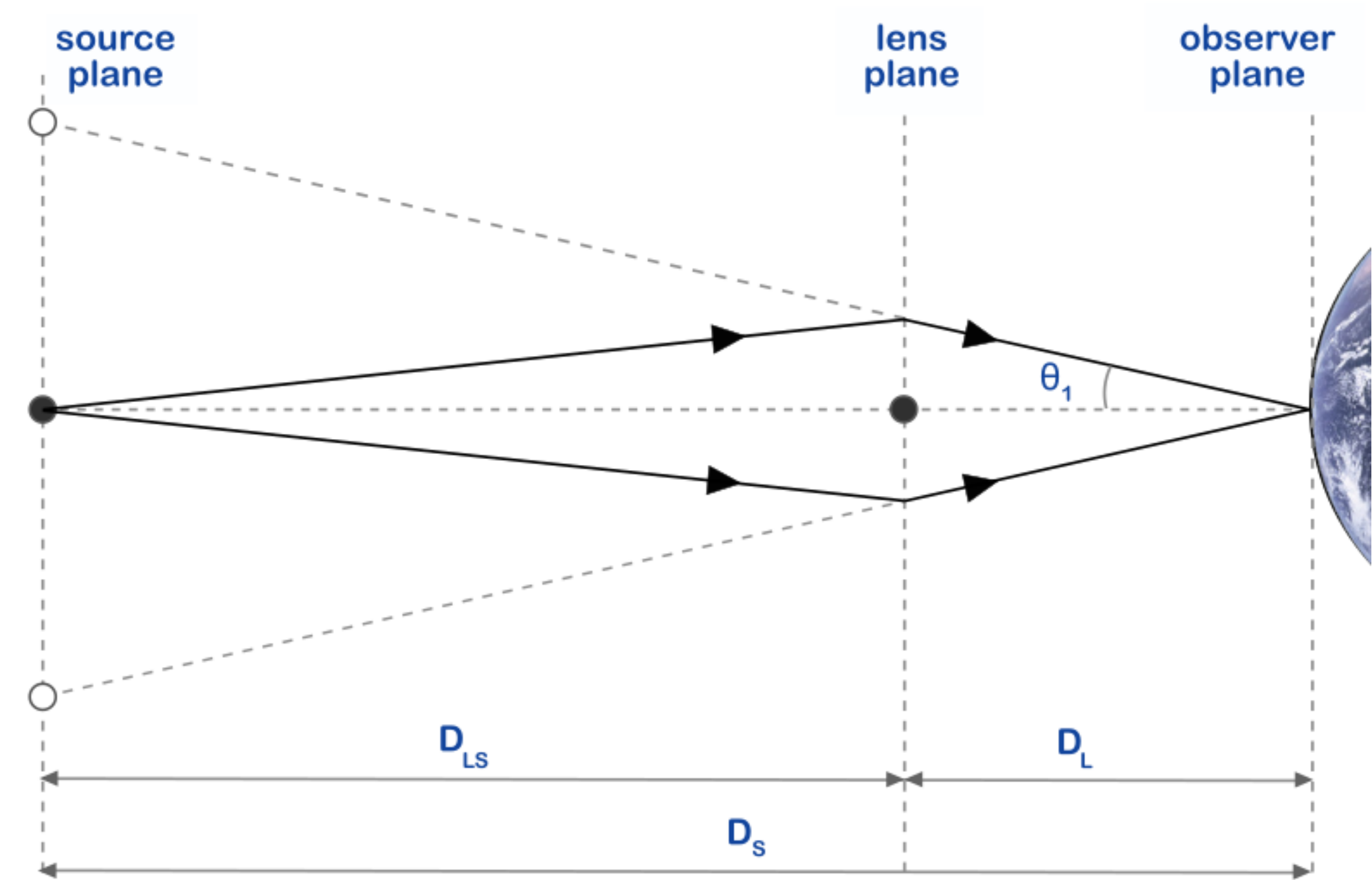
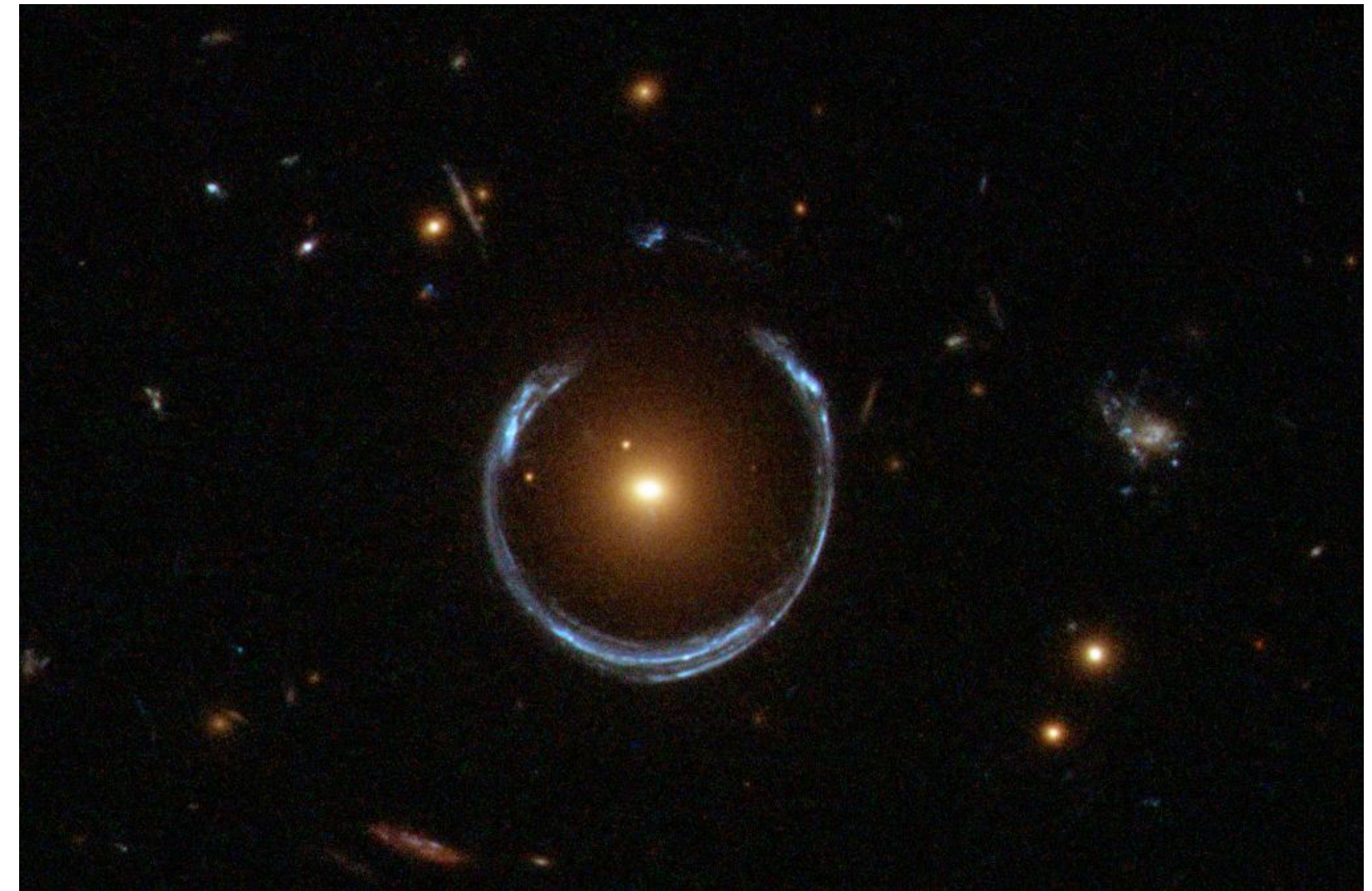
This is in good agreement with a value of  $M = 8.7 \times 10^{11} h^{-1} M_\odot$  obtained with a more accurate treatment of the mass distribution of the lensing galaxy.

# Einstein rings and crosses

If a quasar or other bright source lies exactly along the line of sight to the lensing mass, then it will be imaged as an **Einstein ring** encircling the lens (this phenomenon was described by Einstein in 1936). In this case,  $\beta = 0$  in Fig. 35, and so the angular radius of the Einstein ring is:

$$\theta_E = \sqrt{\frac{4GM}{c^2} \left( \frac{d_S - d_L}{d_S d_L} \right)} \text{ rad.}$$

Of course, **for a point source, the chance of an exact alignment with the lensing mass is essentially zero.** For an extended source, the requirements for an Einstein ring are that  $\beta < \theta_E$  and that **the line of sight through the lensing mass must pierce the extended source.**



# Einstein rings and crosses

Figure 36 shows a calculation of a **partial ring**—the image of a slightly off-center source. The first Einstein ring to be discovered, MG1131+0456, was found at radio wavelengths by the VLA. Figure 37 shows the radio appearance of the ring, which is thought to be the **image of a radio galaxy lensed by an elliptical galaxy**.

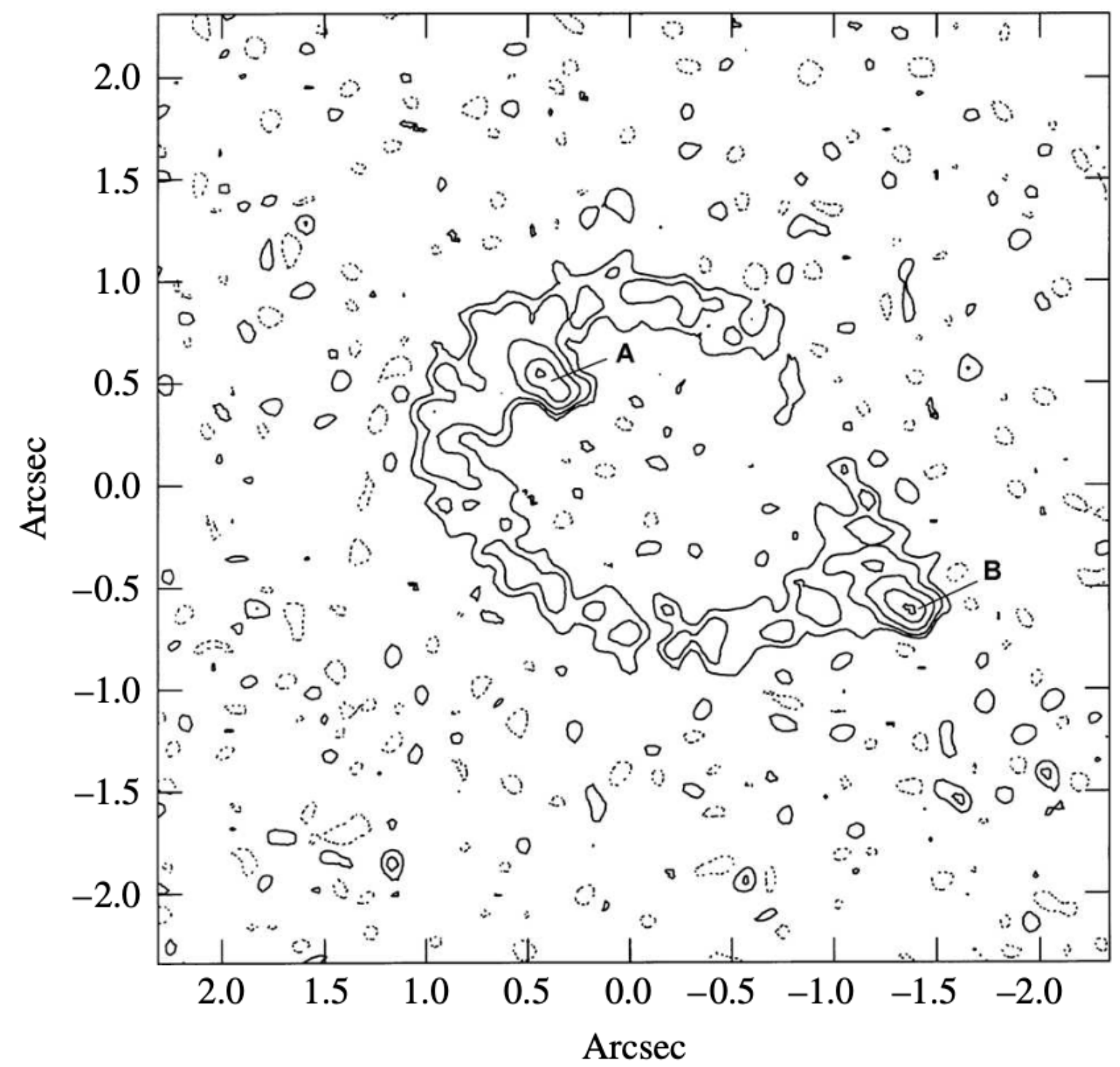


**FIGURE 37** The Einstein ring MG1131+0456. The knot labeled A is produced by the core of the imaged radio galaxy, and the knot labeled B represents one of its lobes. (Figure adapted from Hewitt et al., *Nature*, 333, 537, 1988. Courtesy of J. Hewitt.)

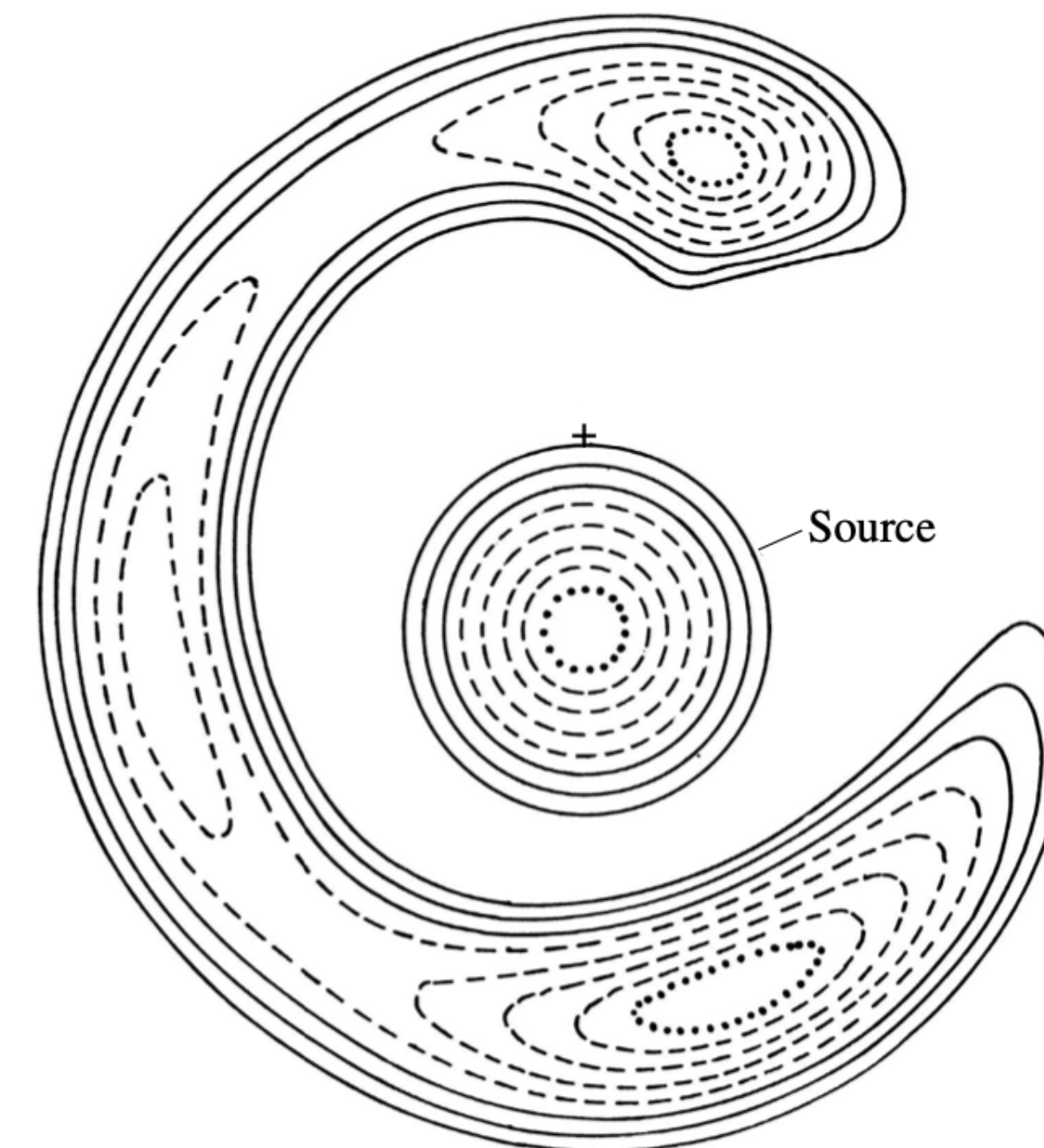
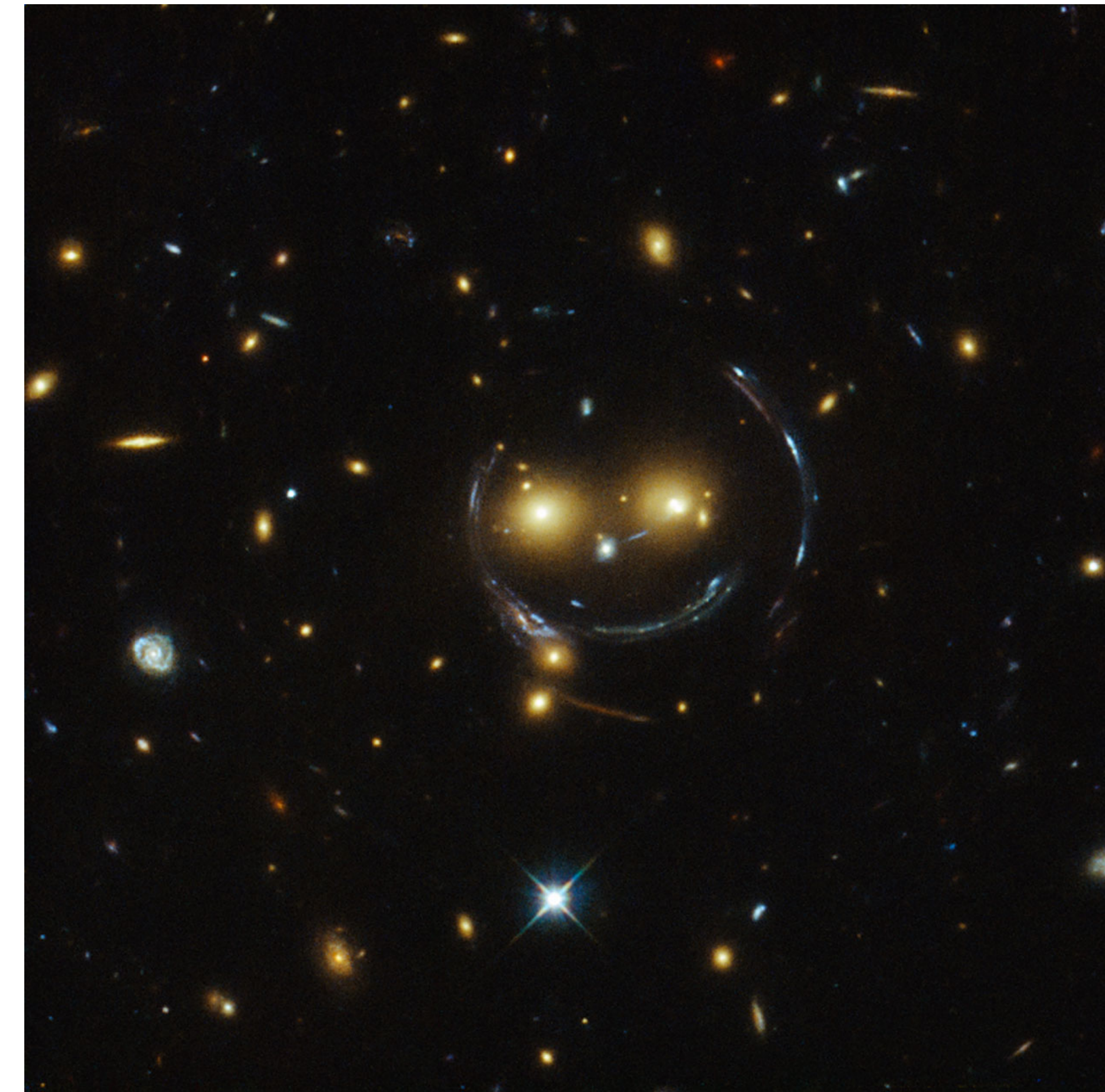
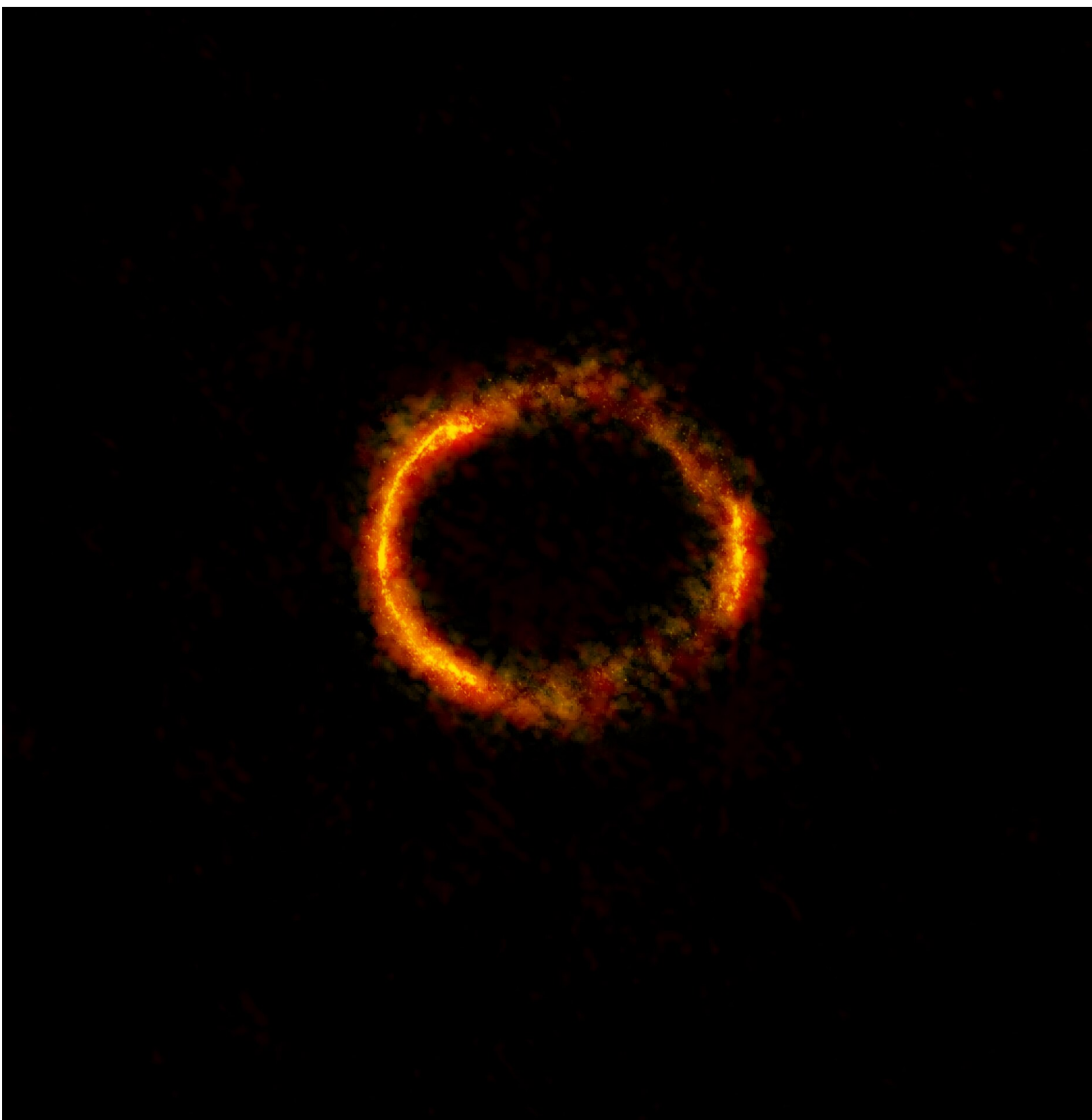


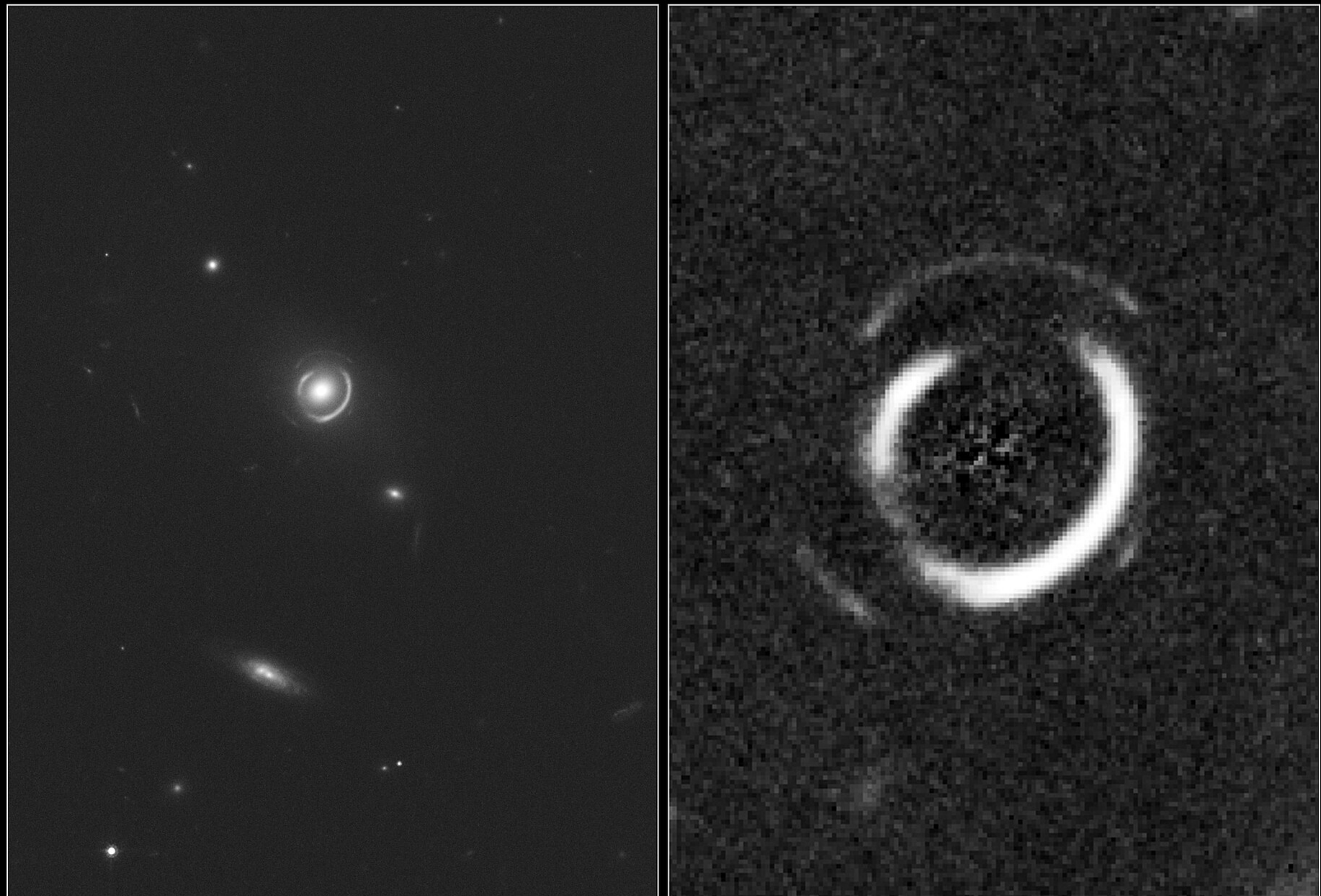
**FIGURE 36** A calculation of the image of a slightly off-center spherical galaxy formed by a lensing mass located at the cross (“+”). (Figure adapted from Chitre and Narasimha, *Gravitational Lenses*, Springer-Verlag, Berlin, 1989.)

# Einstein rings and crosses



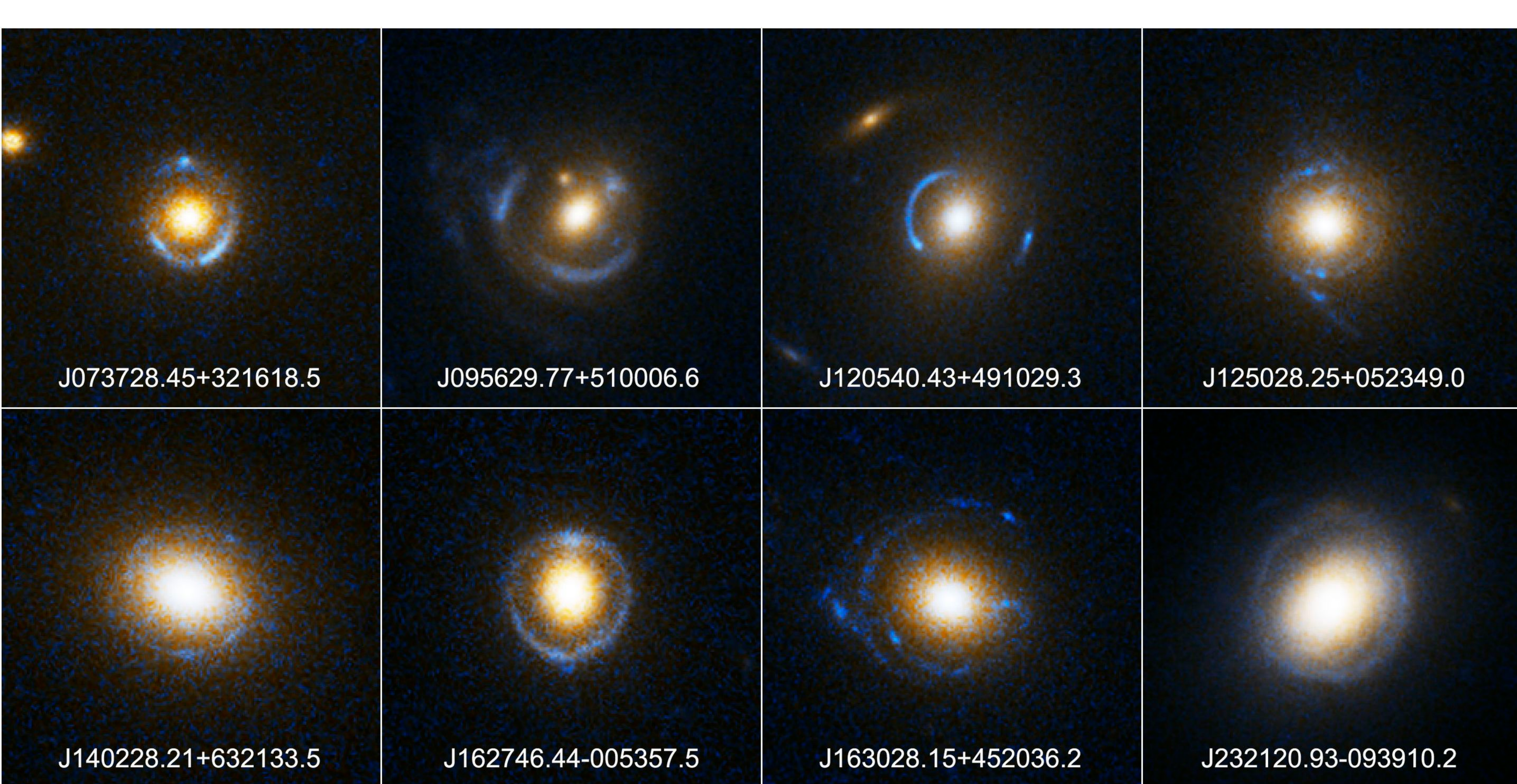
Double Einstein Ring SDSSJ0946+1006

*Hubble Space Telescope* • ACS/WFC



NASA, ESA, R. Gavazzi and T. Treu (University of California, Santa Barbara), and the SLACS Team

STScI-PRC08-04



# Einstein rings and crosses

The value of  $\theta_E$  can be calculated for any gravitational lens, regardless of the alignment of the lens and the source. **Although the image may not be a ring,  $\theta_E$  does provide a useful parameter for describing the properties of any gravitational lens.**

If  $\beta < \theta_E$ , as shown in Fig. 35, there will be **two images formed** by the point mass.

If  $\beta \gg \theta_E$ , the **position and brightness of the source are only slightly altered**, but a **secondary image appears close to the lensing mass** that is **reduced in angular size** by a factor of  $(\theta_E/\beta)^4$ .

A point mass is clearly a crude representation of an actual galaxy. A **better model of the lensing galaxy is provided by an isothermal sphere around a central core**, similar to the model used for the central bulge of the Milky Way. Another improvement is to depart from spherical symmetry and use an **isothermal ellipsoid**, which can **produce either three or five images** (an extended distribution of mass will produce an odd number of images).

# Einstein rings and crosses

The **Einstein cross** shown in Fig. 38 includes **four images of a distant quasar** (Q2237+031, at  $z = 1.69$ ) that is **lensed by a nearby ( $z = 0.04$ ) spiral galaxy**. There is probably also a **fifth faint central image that is overwhelmed by the lensing galaxy at the center** of the cross. Note that image A has brightened by 0.5 mag in the 3-year interval between the photos.

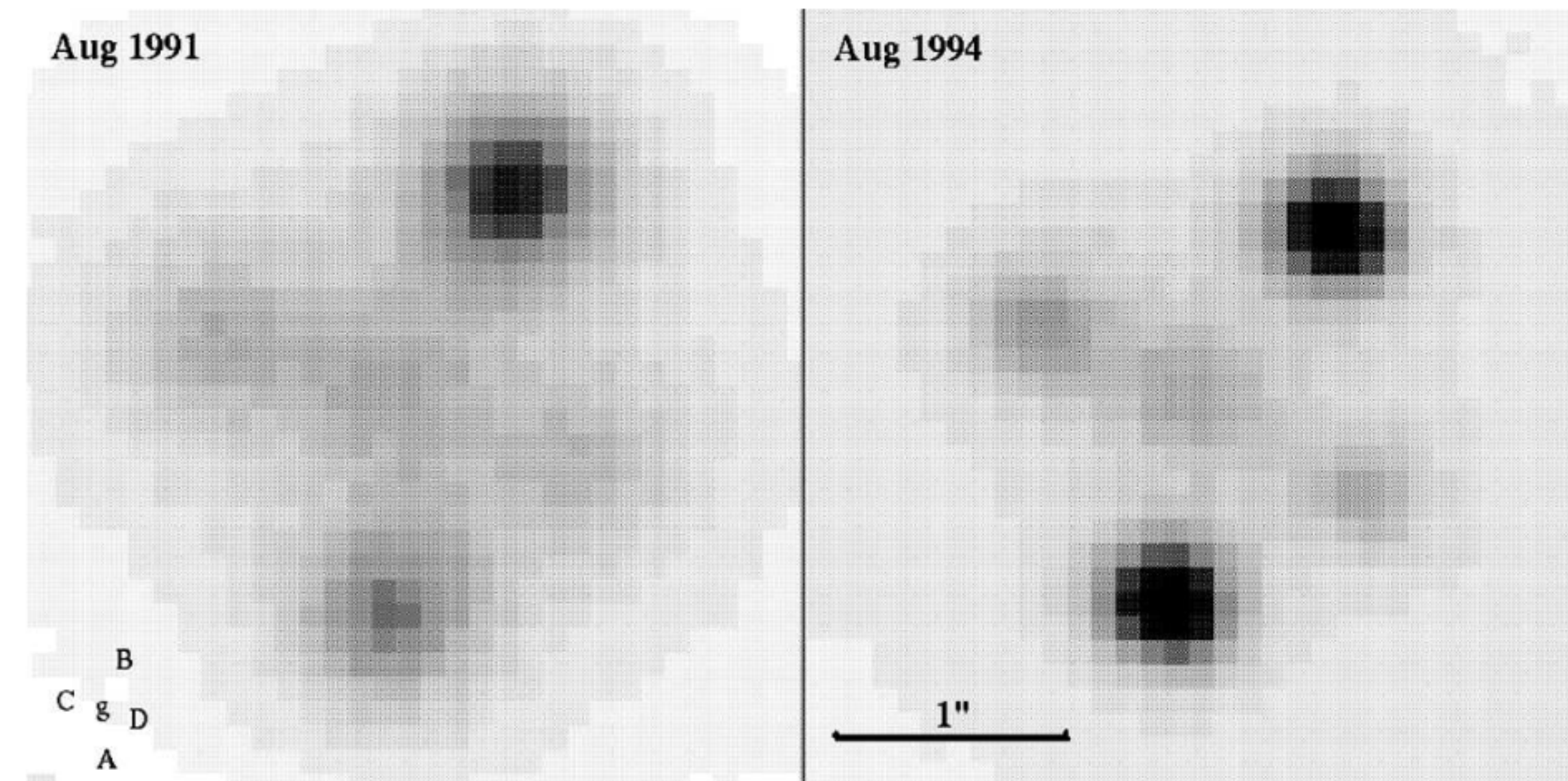
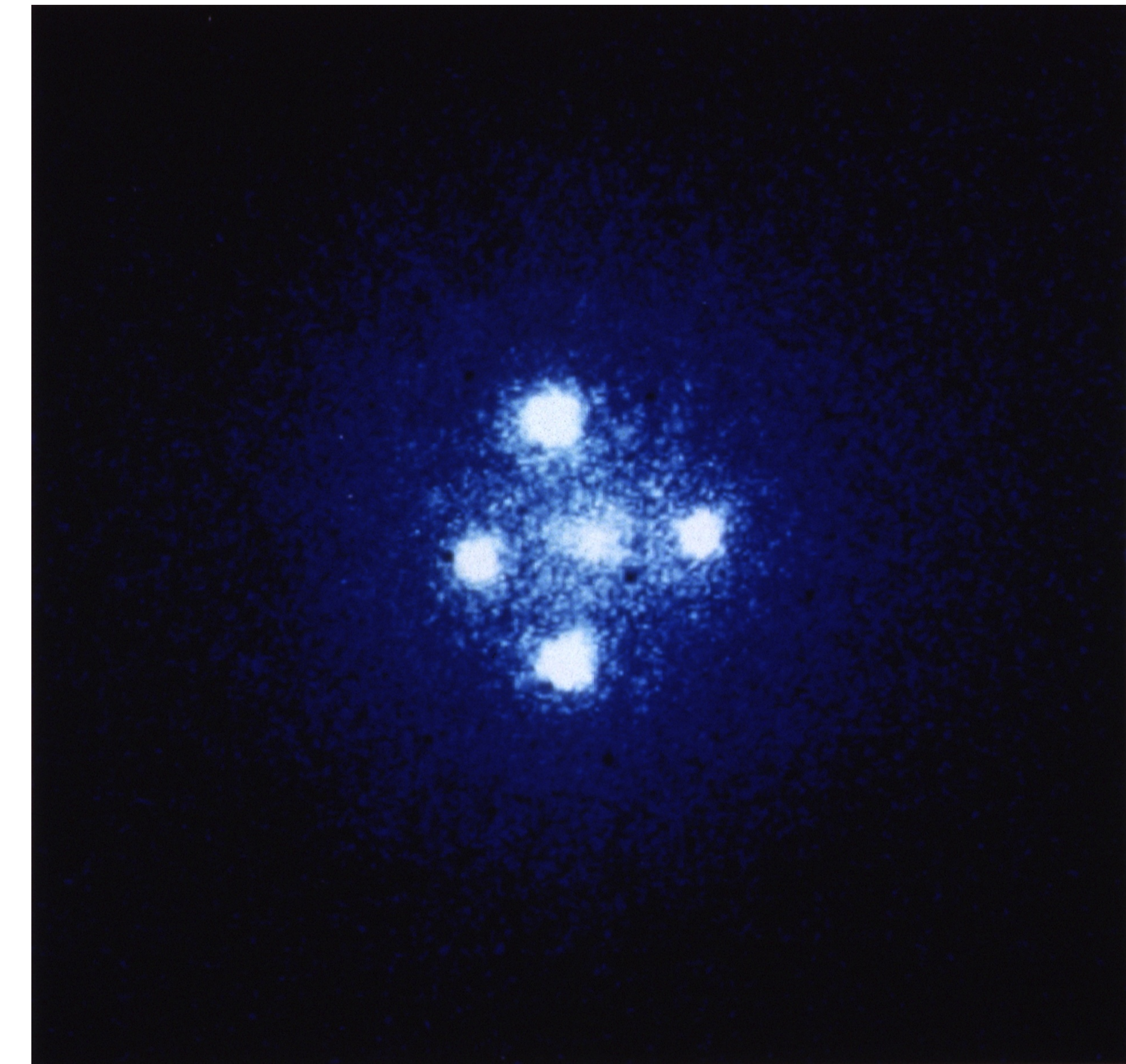
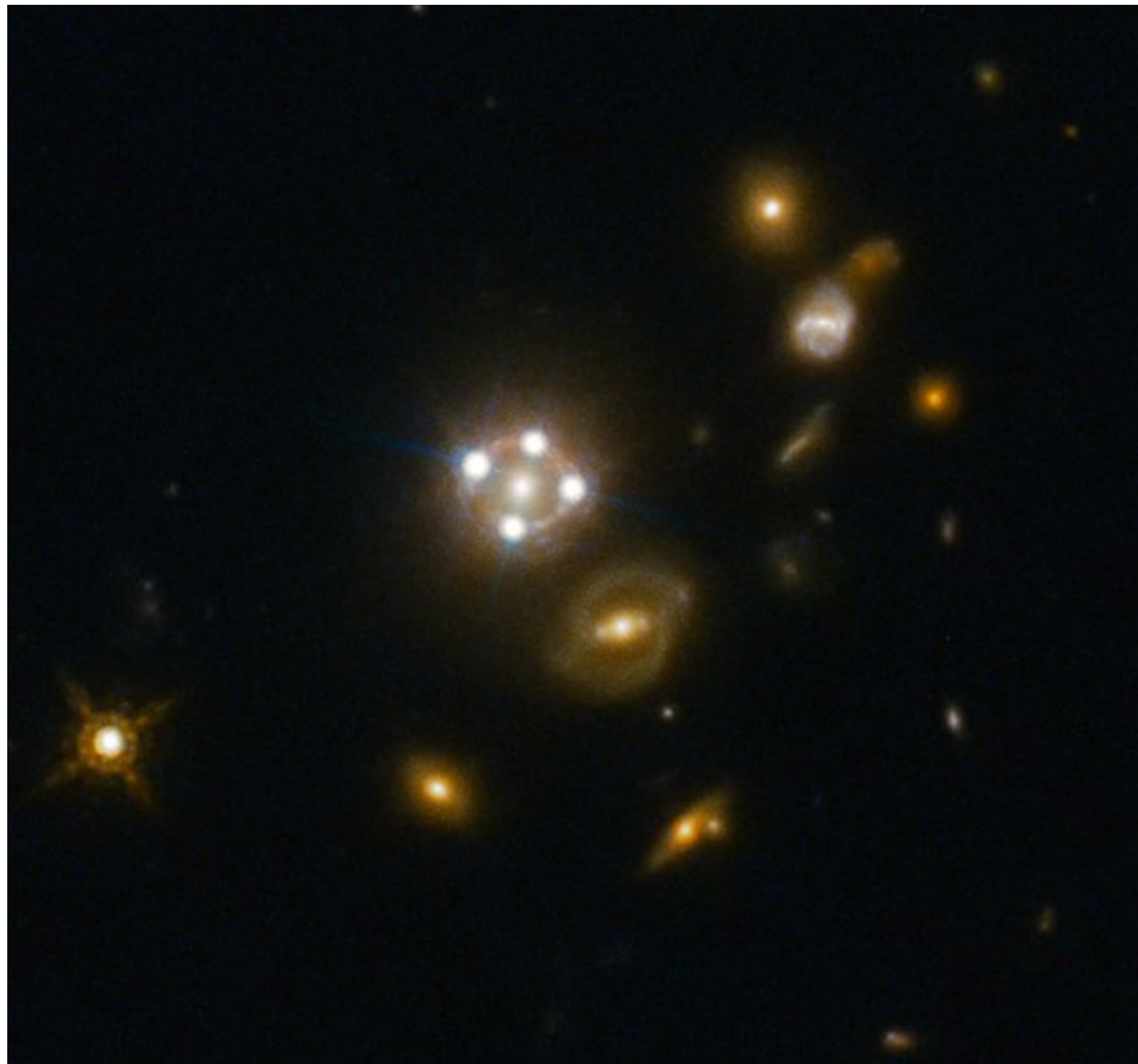


**FIGURE 38** The Einstein cross Q2237+031, as observed in August 1991 (left) and August 1994 (right). The cross consists of 4 images of the quasar (labeled A–D), with the lensing galaxy (labeled g) at the center. (Courtesy of Geraint Lewis and Mike Irwin.)

# Einstein rings and crosses



# Arcs in galaxy clusters

Another example of gravitational lensing is the formation of **arcs** by light passing through a cluster of galaxies.

One such arc in the cluster **Abell 370** is shown in Fig. 39. Up to **60 additional “arclets”** and **several distorted distant background galaxies have also been observed in that cluster.**

The source of **the large arc must be a resolved object such as a galaxy** rather than the starlike nucleus of a quasar.



# Arcs in galaxy clusters

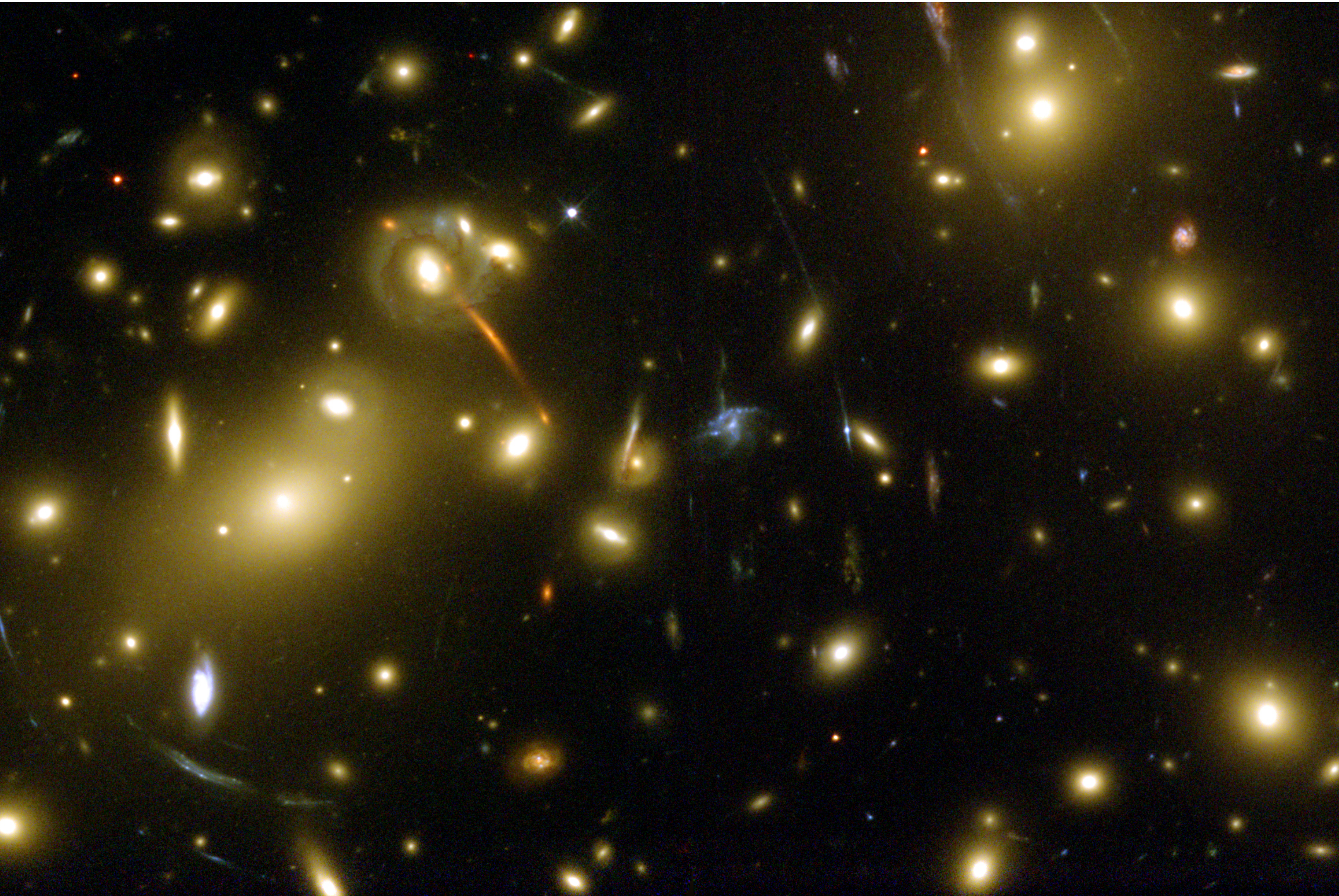
According to one model of Abell 370, the lensing mass (visible galaxies and dark matter) needed to produce the images is about  $5 \times 10^{14} M_{\odot}$ . Taken with the combined luminosity of a few  $\times 10^{11} L_{\odot}$  for the lensing galaxies, this implies a **mass-to-light ratio of at least 1000  $M_{\odot}/L_{\odot}$ , indicating the presence of large amounts of dark matter.**

Abell 370 is an unusual **cluster** in that it is **sufficiently centrally condensed to produce such arcs**. The dark matter in most clusters is probably more widely distributed, producing weak lensing effects just strong enough to distort the appearance of distant galaxies seen beyond the cluster.



# Arcs in galaxy clusters

A spectacular example of **multiple arclets that are lensed images of background galaxies** produced by the cluster Abell 2218. Such weak lensing can also cause an apparent bunching of quasars, so statistical studies of the clustering of objects in the very early universe must take this effect into account.



# Time variability of multiple images

An interesting effect occurs when the source for a pair of images increases its luminosity. Because the light from the source takes different paths on its way to the observer, there will be a **time delay between the brightening of the lensed images**. A time delay of about **1.4–1.5 yr has been measured** for the original double quasar, Q0957+561. Nonperiodic celestial events usually catch astronomers by surprise, but this time delay puts astronomers in the unique situation of knowing in advance how a lensed quasar will behave.

It turns out that the **time delay is also inversely proportional to the Hubble constant**. This offers a way of **determining the value of  $H_0$**  that is independent of any other distance measurement. At the cosmological distances of quasars, their recessional velocities should completely dominate their peculiar velocities through space. One study using Q0957+561 concluded that  $H_0 = 69 \pm 21 \text{ km s}^{-1} \text{ Mpc}^{-1}$ , assuming that the lensing galaxy contains a substantial amount of dark matter. The result is in excellent agreement with the WMAP value of  $H_0 = 71 \pm 4 \text{ km s}^{-1} \text{ Mpc}^{-1}$ .

# The Lyman-Alpha forest

The spectra of high-redshift quasars always display a large number of narrow absorption lines superimposed on the quasar's continuous spectrum (these lines are in addition to any broad absorption lines that are associated with the quasar itself). These **narrow lines are formed when the light from a quasar passes through material** (an interstellar cloud, a galactic halo) that **happens to lie along the line of sight**. If the absorbing material is far from Earth, its recessional motion will cause these absorption lines to be strongly redshifted. Furthermore, if **the light passes through more than one cloud or galactic halo, different sets of absorption lines** will be seen. Each set of lines corresponds to the redshift of a particular cloud or halo.

**There are two classes of narrow absorption lines in quasar spectra:**

- The **Lyman- $\alpha$  forest** is a dense thicket of **hydrogen absorption lines**. These lines are believed to be formed in **intergalactic clouds** and display a variety of redshifts. Absorption by primordial ionized helium (He II) has also been detected.
- Lines are also formed by **ionized metals**, primarily **carbon (C IV) and magnesium (Mg II)**, together with silicon, iron, aluminum, nitrogen, and oxygen. The mix of elements is similar to that found in the interstellar medium of the Milky Way, indicating that the material has been processed through stars and enriched in heavy elements. These lines are thought to be **formed in the extended halos or disks of galaxies found along the line of sight to the quasar**.

# The Lyman-Alpha forest

Most of these lines are **normally found at ultraviolet wavelengths**, when the absorbing material is moving at a small fraction of the speed of light relative to Earth (i.e., has a small redshift). They are rarely seen from the ground because Earth's atmosphere absorbs most ultraviolet wavelengths. However, if the absorbing material is receding fast enough, the **Doppler effect can shift ultraviolet lines to visible wavelengths**, where the atmosphere is transparent. For this reason, these **absorption lines are seen from the ground only in the spectra of highly redshifted quasars**.

# The Lyman-Alpha forest

**Example 4.2.** The rest wavelength of the ultraviolet Lyman- $\alpha$  line of hydrogen is  $\lambda_{\text{Ly}\alpha} = 121.6 \text{ nm}$ . To determine the redshift required to bring this line into the visible region of the electromagnetic spectrum, we can use the definition of  $z$ ,

$$z = \frac{\lambda_{\text{obs}} - \lambda_{\text{rest}}}{\lambda_{\text{rest}}}.$$

Using  $\lambda_{\text{rest}} = \lambda_{\text{Ly}\alpha}$  and  $\lambda_{\text{obs}} = 400 \text{ nm}$  for the blue end of the visible spectrum, we require a redshift of

$$z > \frac{400 \text{ nm} - 121.6 \text{ nm}}{121.6 \text{ nm}} \simeq 2.3,$$

just to bring the Ly $\alpha$  line to the edge of the visible spectrum. Actually, some near-ultraviolet light can penetrate Earth's atmosphere, so the **Ly $\alpha$  line can be observed when  $z > 1.7$  for the absorbing material.**

# The Lyman-Alpha forest

Typically, the spectrum of a high-redshift quasar contains a **strong Lyman- $\alpha$  emission line produced by the quasar itself**, and perhaps some **50 Ly $\alpha$  absorption lines at shorter wavelengths** (smaller redshifts); see Fig. 41. Each one of these lines is from a **different intergalactic cloud of hydrogen** encountered by the quasar's continuum radiation.

**The Ly $\alpha$  line profile can be used to calculate the column density of the neutral hydrogen atoms in the cloud that produces each line.** A typical result is  $10^{18} \text{ m}^{-2}$ . In other words, a hollow tube having a cross-sectional area of  $1 \text{ m}^2$  that crossed completely through the cloud would contain  $10^{18}$  neutral hydrogen atoms.

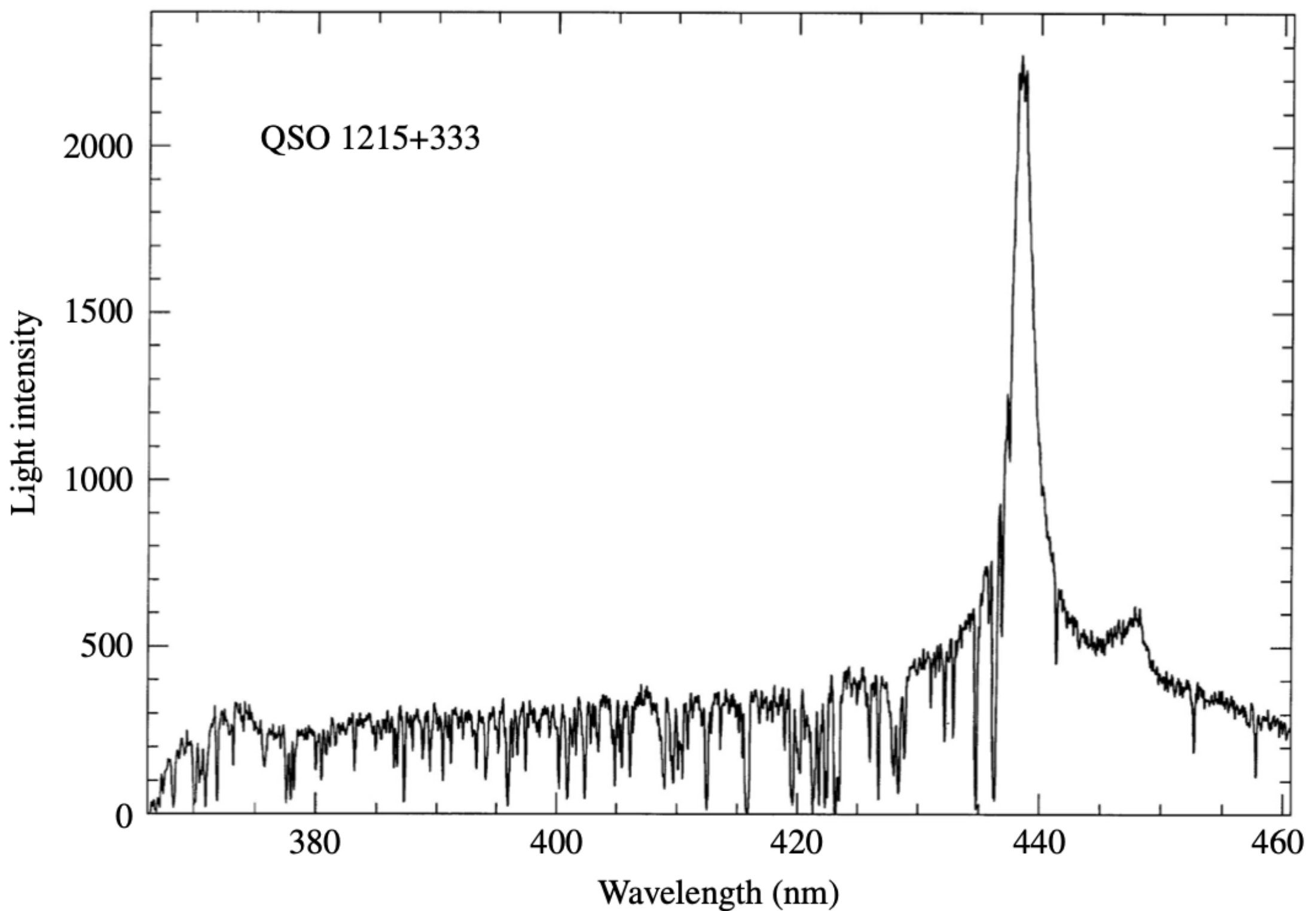


**FIGURE 41** The strong Ly $\alpha$  emission line in the spectrum of QSO 1215+333, with the Ly $\alpha$  forest of absorption lines at shorter wavelengths. (Adapted from a figure courtesy of J. Bechtold, Steward Observatory, University of Arizona.)

# The Lyman-Alpha forest

Such a cloud would be extremely **transparent to the ultraviolet radiation** that is normally present throughout space. As a result, this ultraviolet background can penetrate the **cloud and keep it almost completely ionized**. Calculations indicate that only one hydrogen atom in  $10^5$  remains neutral in the cloud and is capable of absorbing an ultraviolet photon.

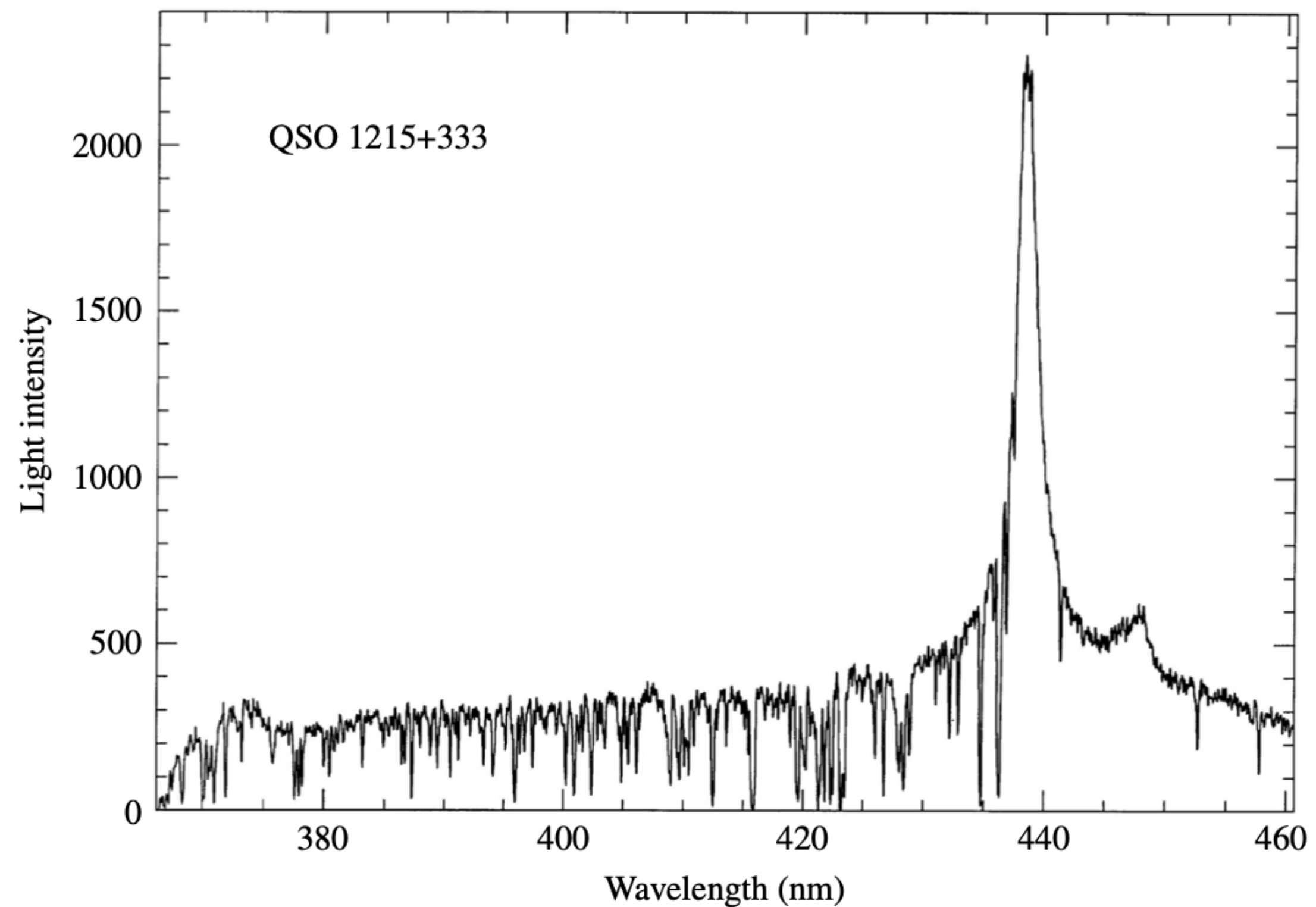


**FIGURE 41** The strong Ly $\alpha$  emission line in the spectrum of QSO 1215+333, with the Ly $\alpha$  forest of absorption lines at shorter wavelengths. (Adapted from a figure courtesy of J. Bechtold, Steward Observatory, University of Arizona.)

# The Lyman-Alpha forest

We deduce the size of the intergalactic clouds by comparing the Ly $\alpha$  forest in the spectra of pairs of lensed quasars. Many of the absorption lines are seen in both spectra, but some are not. This indicates that the clouds are, on average, about the size of the lensing galaxy. From the total calculated column density of hydrogen (ionized as well as neutral), the mass of a typical cloud probably lies between  $10^7$  and  $10^8 M_{\odot}$ . At the temperature estimated for a typical cloud by some astronomers (approximately  $3 \times 10^4$  K), its self-gravity would be too weak to keep it from dispersing. It may be held together by the pressure of a less dense (but hotter) external intergalactic medium or by the presence of dark matter within the cloud.

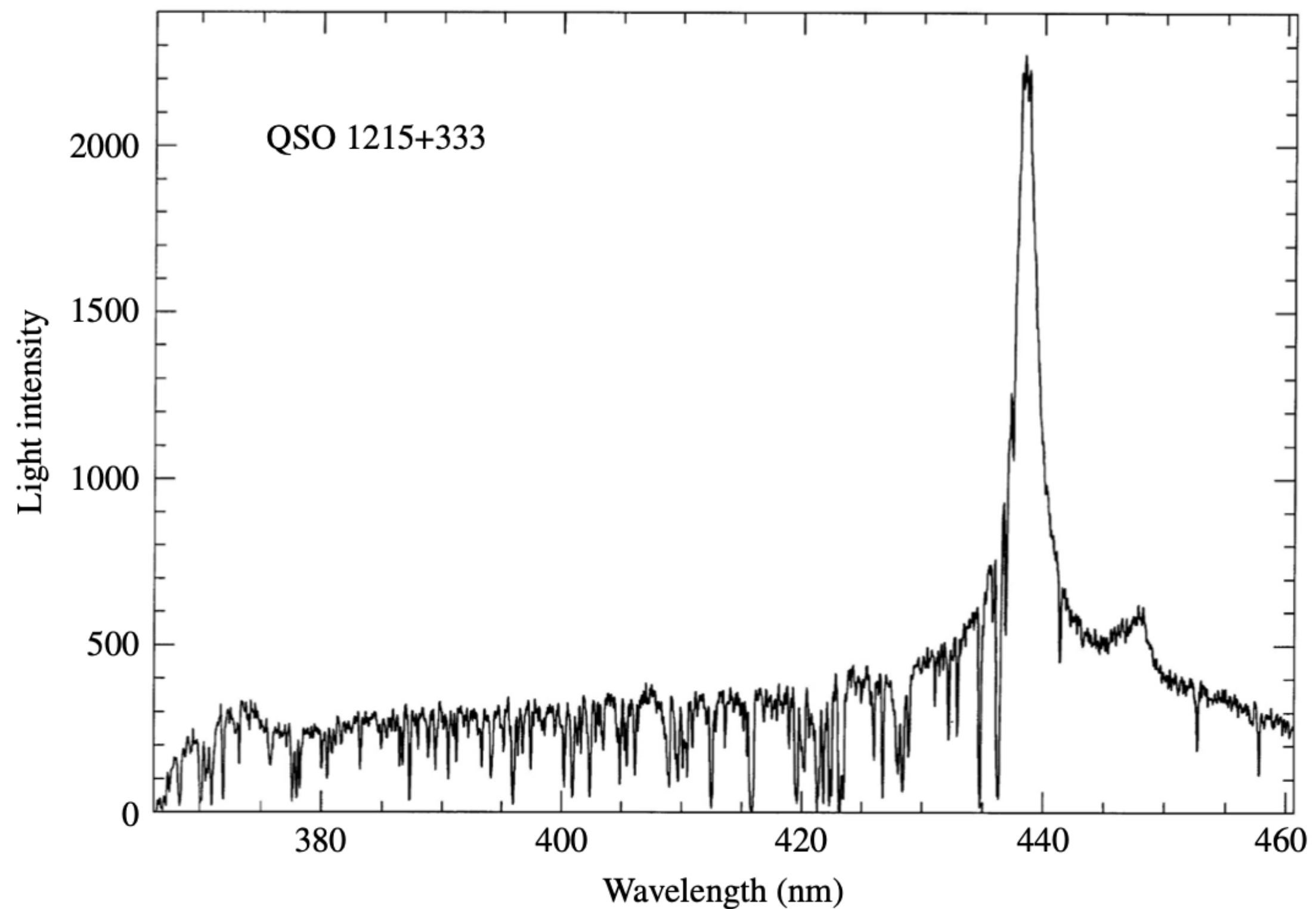


**FIGURE 41** The strong Ly $\alpha$  emission line in the spectrum of QSO 1215+333, with the Ly $\alpha$  forest of absorption lines at shorter wavelengths. (Adapted from a figure courtesy of J. Bechtold, Steward Observatory, University of Arizona.)

# Ionised metal absorption lines

The **narrow absorption lines produced by ionized metals in quasar spectra have a different origin**. They can be divided into **two groups** as observed from Earth's surface, corresponding to **two different redshift ranges**.

**Below roughly  $z = 1.5$ , the Mg II lines dominate**, accompanied by Si II, C II, Fe II, and Al II, because they fall within the wavelength window that can be seen from the ground (the Mg II lines are probably produced in the **halos of normal galaxies or in regions of star formation**.).

The **C IV lines**, together with Si IV, N V, and O IV, are common between about  **$z = 1.2$  and  $z = 3.5$** , however.

The distribution of redshifts of these lines is in general agreement with the expected **distribution of galaxies at that earlier time when the universe was smaller** by a factor of  $1 + z$ , assuming that the galactic halos are typically some 30–50 kpc across. In fact, some Mg II systems with  $z < 1$  have been clearly identified with foreground galaxies seen in direct images. The **C IV lines** probably come from **clouds in young galaxies that are strongly ionized by young, hot OB stars**. These narrow metal lines indicate **lower-than-solar abundances of heavy elements**, consistent with their origin in **young galaxies** that may still be in the process of forming.

# What is happening here?



**Hanny's Voorwerp**

[https://en.wikipedia.org/wiki/Hanny%27s\\_Voorwerp](https://en.wikipedia.org/wiki/Hanny%27s_Voorwerp)

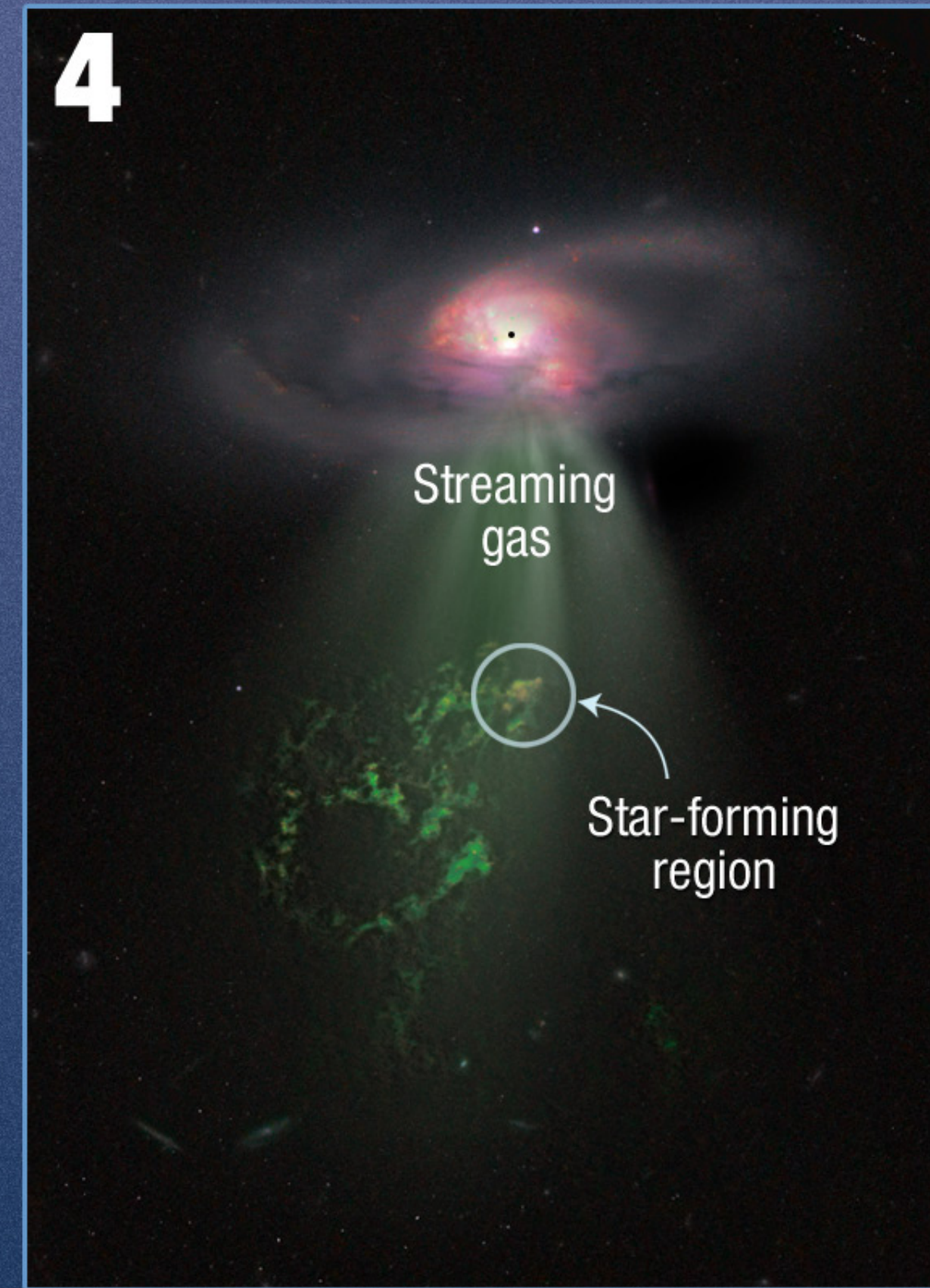
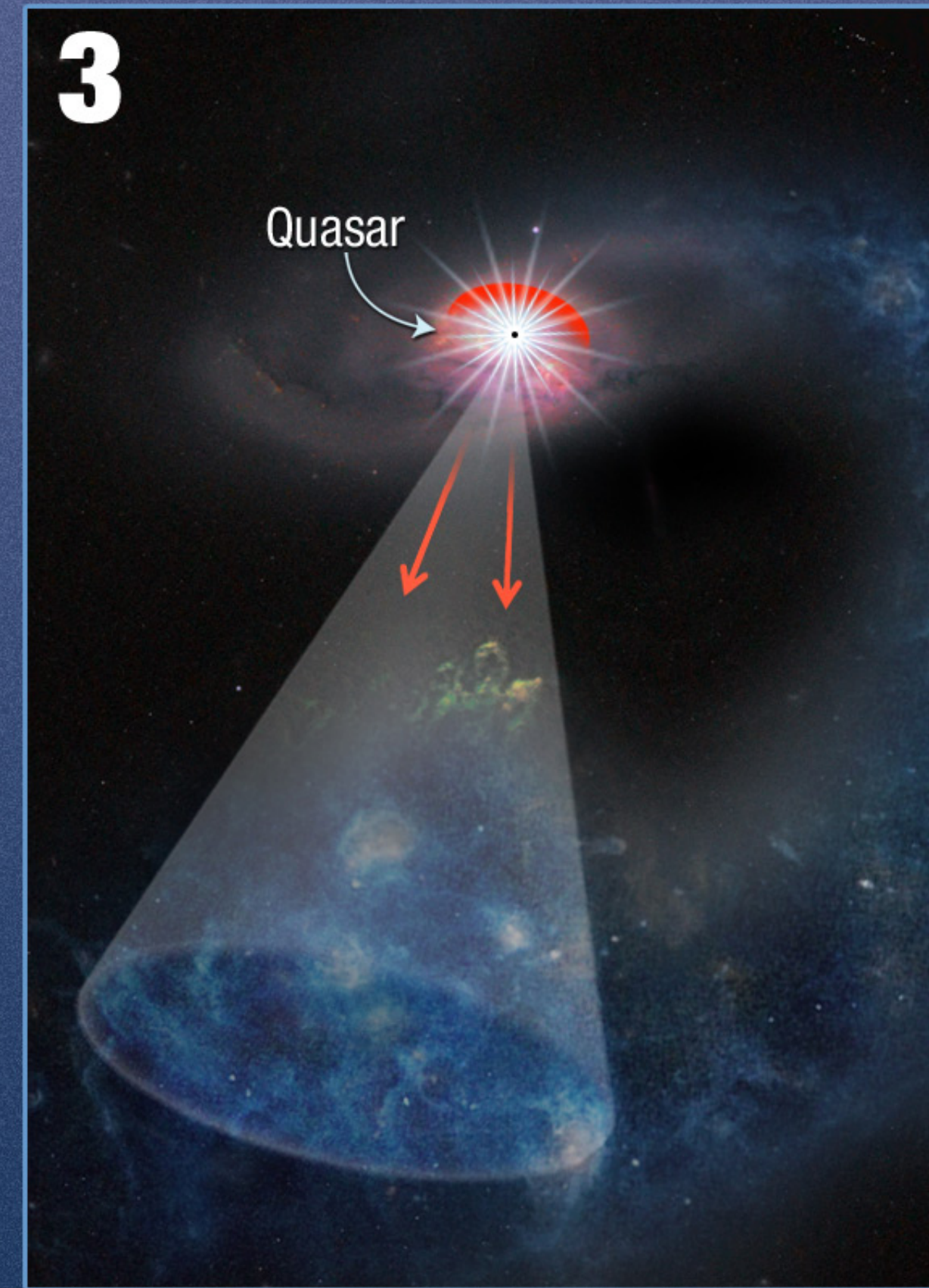
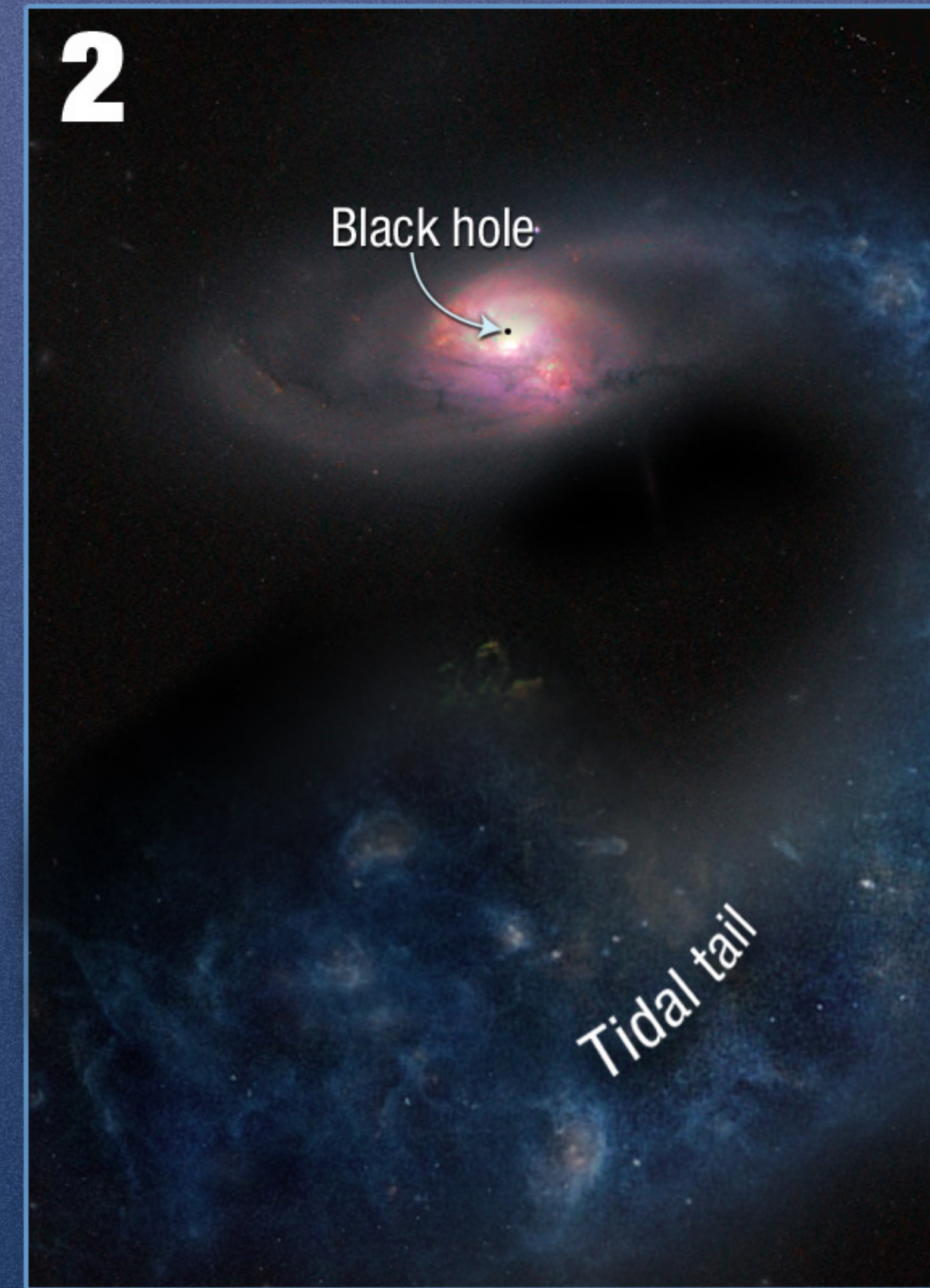
# What is happening here?

**Hanny's Voorwerp**  
**A quasar**  
**ionisation echo**

[https://en.wikipedia.org/wiki/Hanny%27s\\_Voorwerp](https://en.wikipedia.org/wiki/Hanny%27s_Voorwerp)



# Hanny's Voorwerp\* — A Space Oddity



Spiral galaxy IC 2497 gravitationally interacts with a bypassing galaxy.

A large tidal tail of gas is pulled out of the spiral galaxy.

Engorged with gas, a black hole at the center of IC 2497 "turns on" as a quasar and emits a powerful cone of light, which ionizes a portion of the tidal tail, creating Hanny's Voorwerp.

Gas streaming out from the galaxy's center impacts the tidal tail and triggers star formation.

\*Hanny's Object

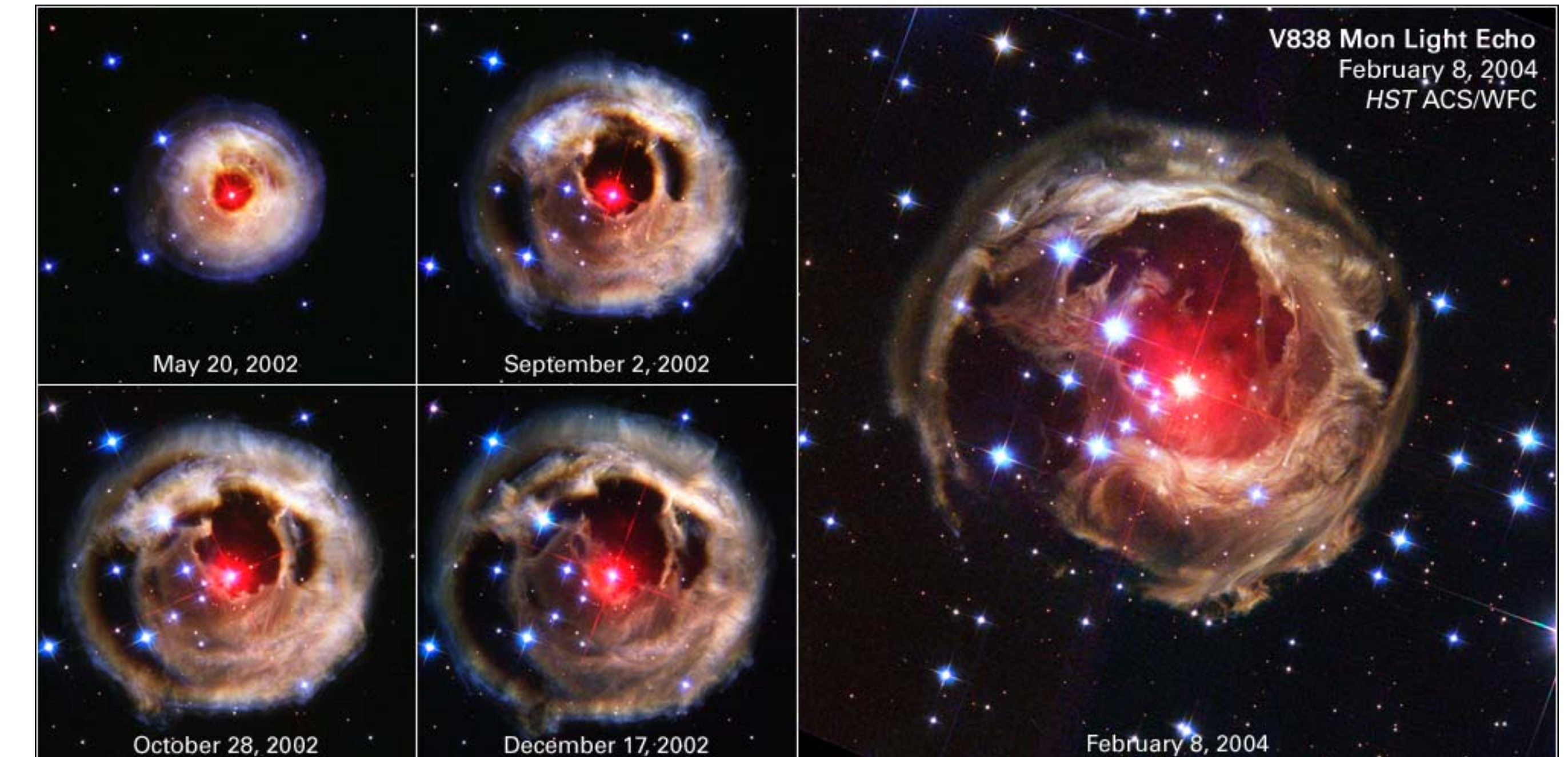
# Light echoes

A light echo is a physical phenomenon caused by **light reflected off surfaces distant from the source**, and **arriving at the observer with a delay relative to this distance**. The phenomenon is analogous to an echo of sound, but due to the much faster speed of light, it mostly only manifests itself over astronomical distances.

For example, a light echo is produced when a **sudden flash** from a nova is **reflected off a cosmic dust cloud**, and arrives at the viewer after a longer duration than it otherwise would have taken with a direct path.

Because of their geometries, light echoes can produce the illusion of superluminal motion.

**Variable star  
V838 Mon**

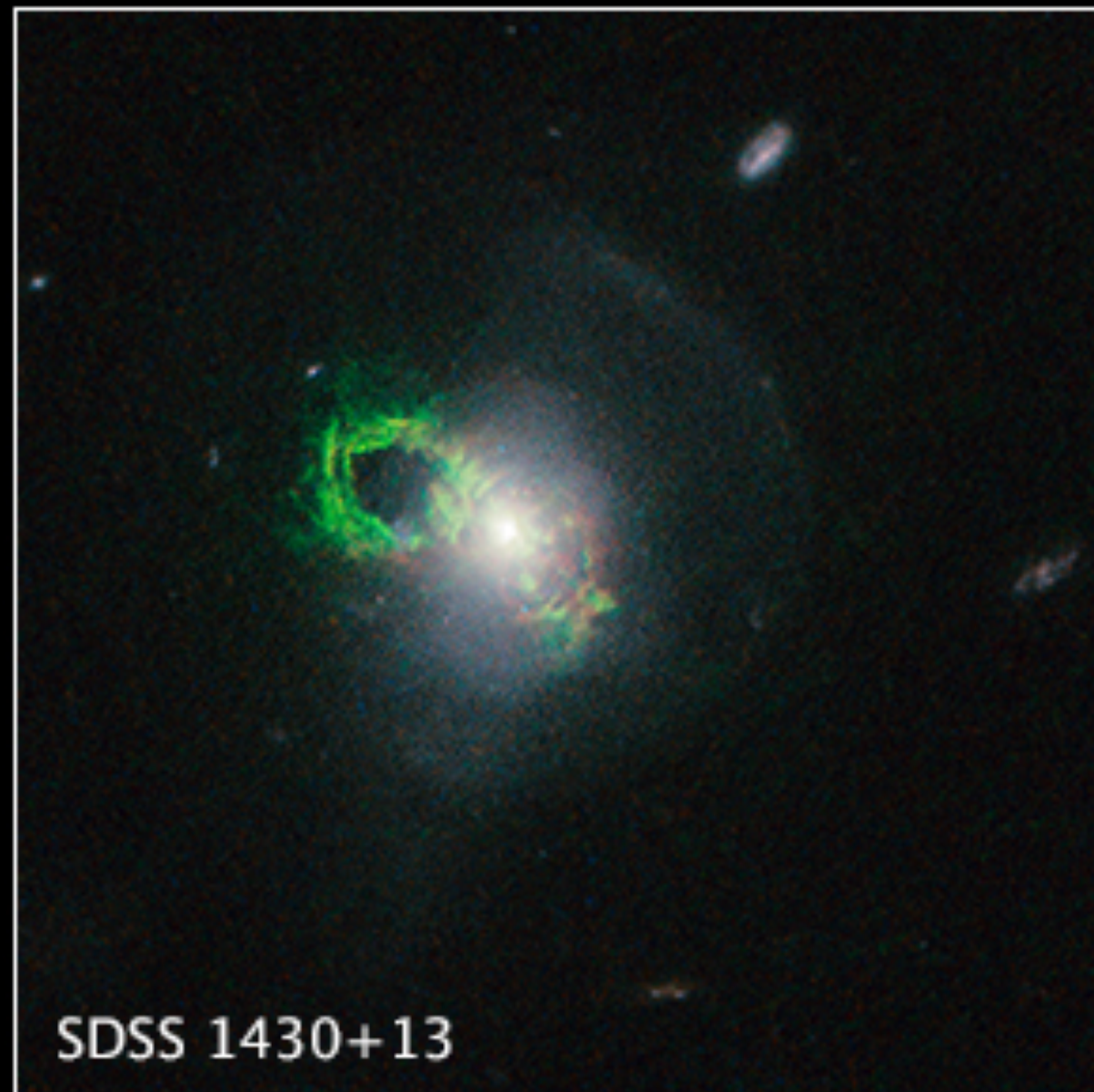


# Light echos - RS Pupis

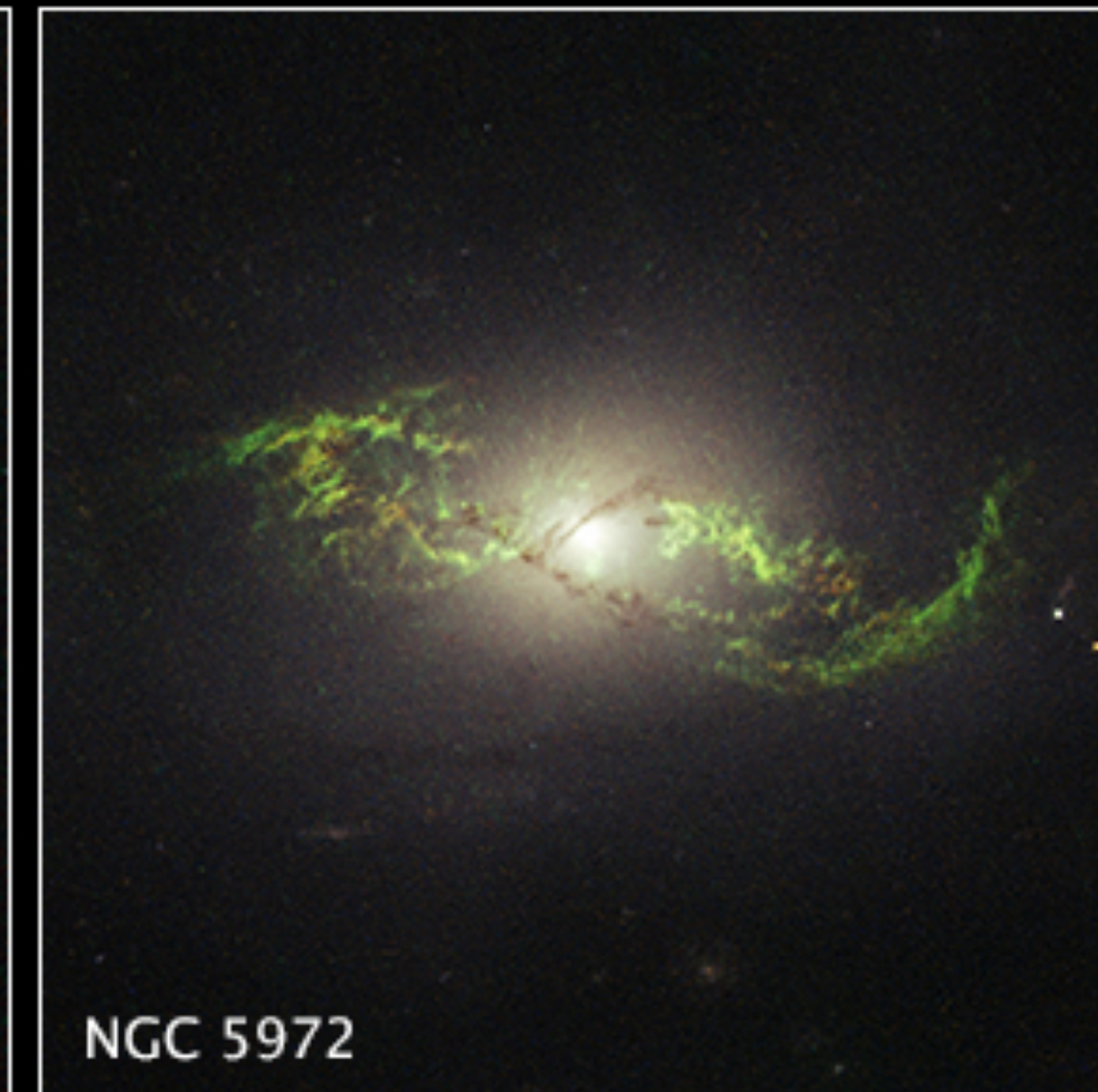


[www.spacetelescope.org](http://www.spacetelescope.org)

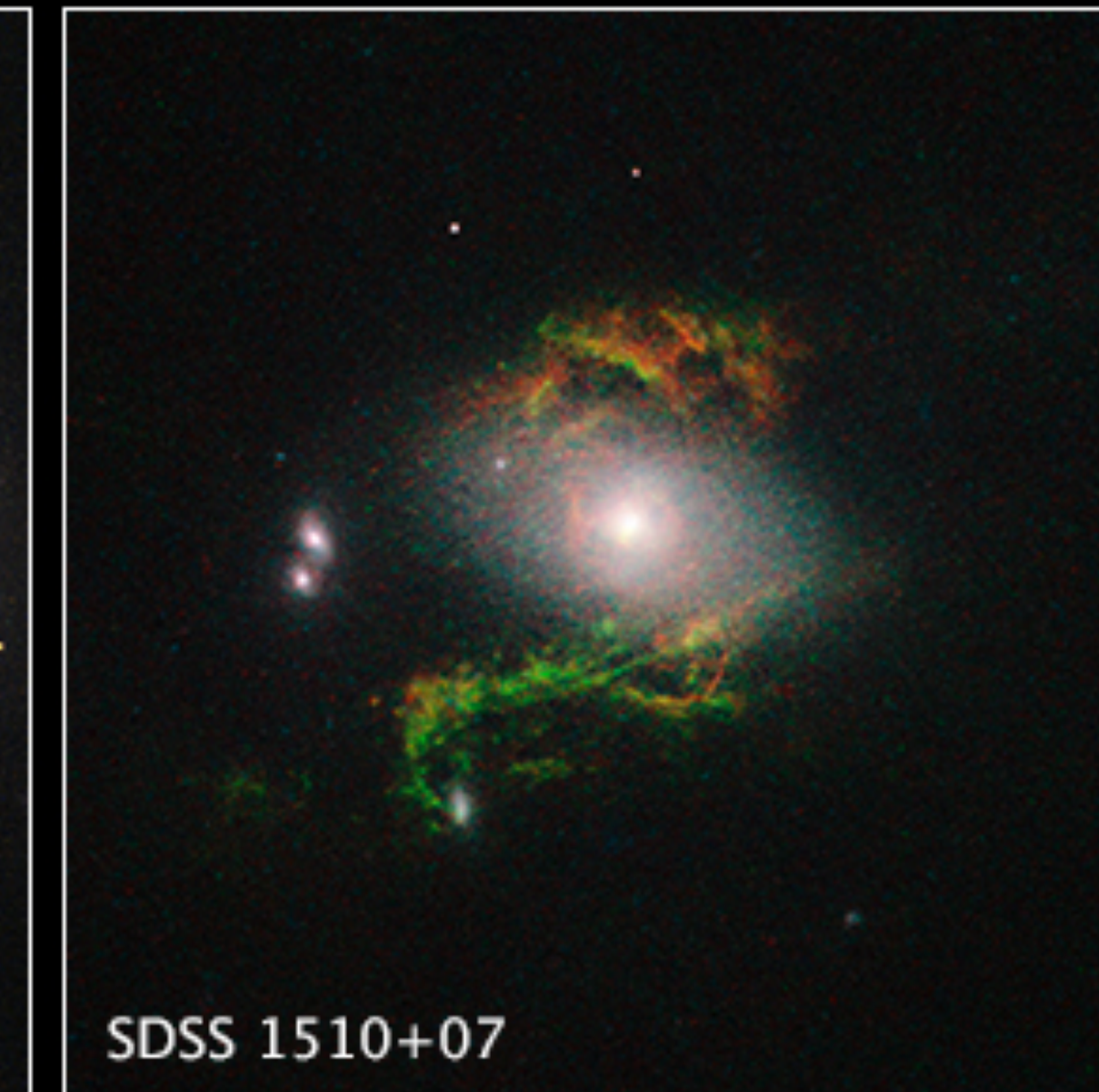
# Extended Gas in Active Galaxies ▪ Hubble Space Telescope ▪ WFPC2 ▪ ACS/WFC ▪ WFC3/UVIS



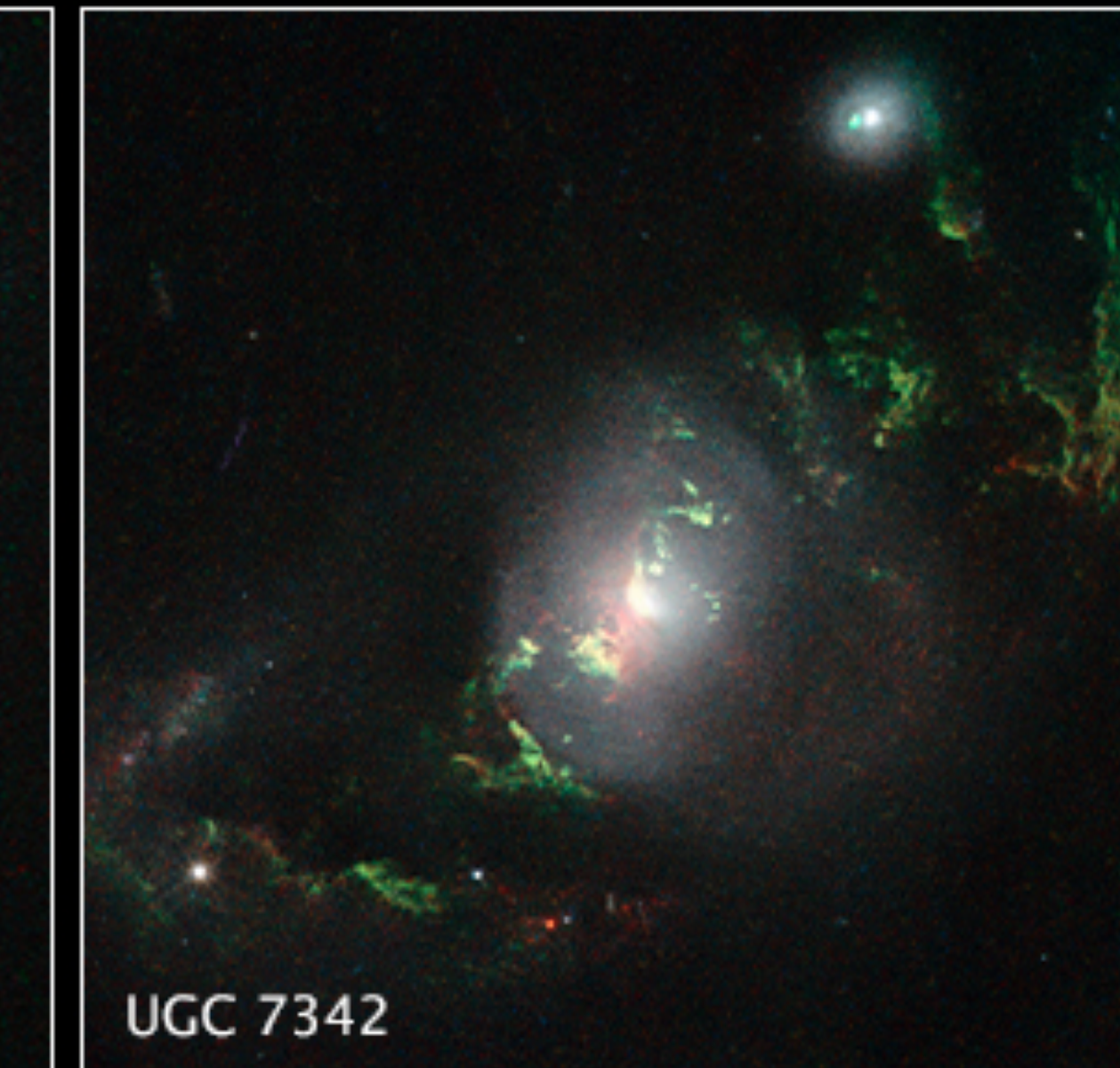
SDSS 1430+13



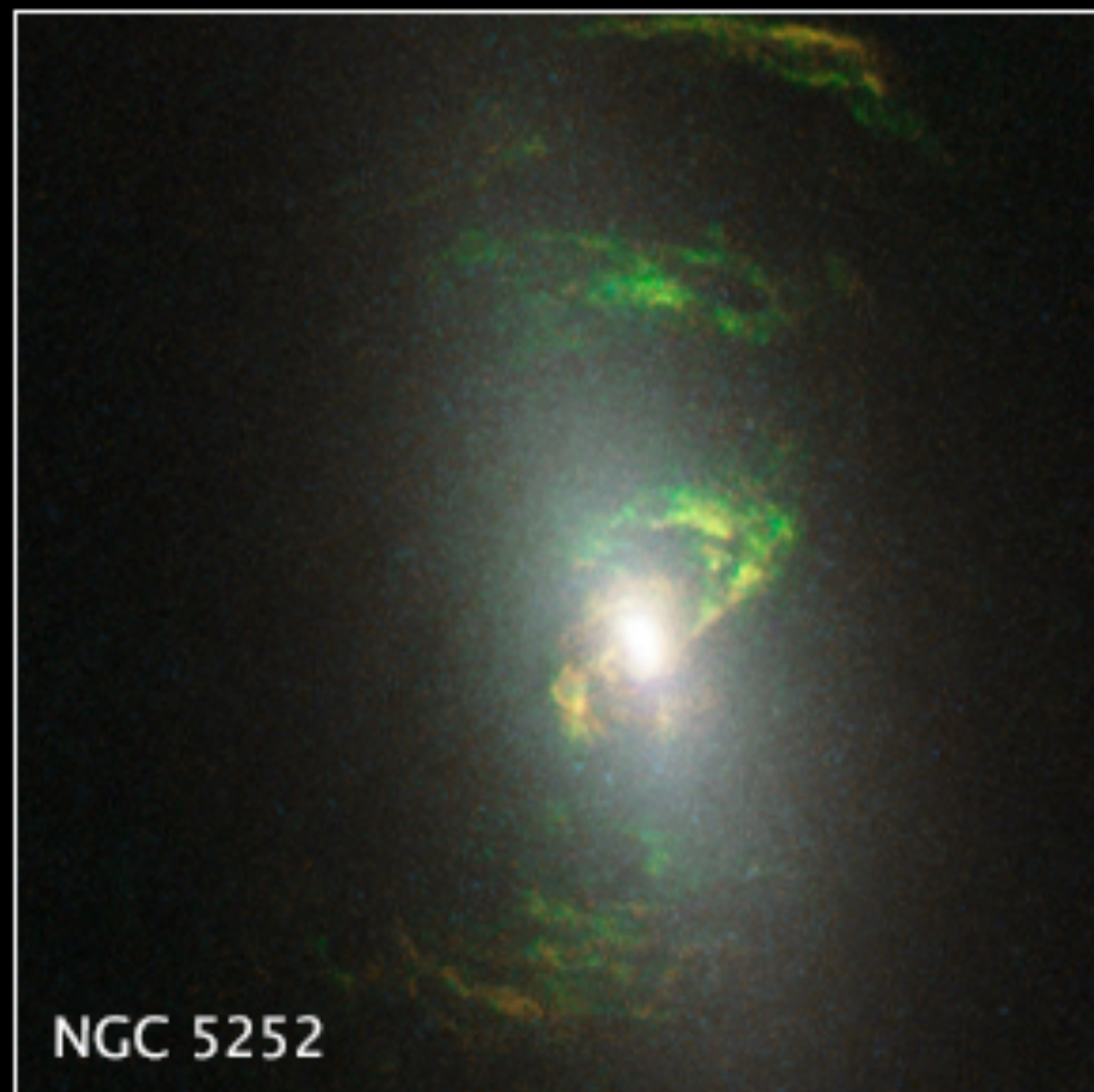
NGC 5972



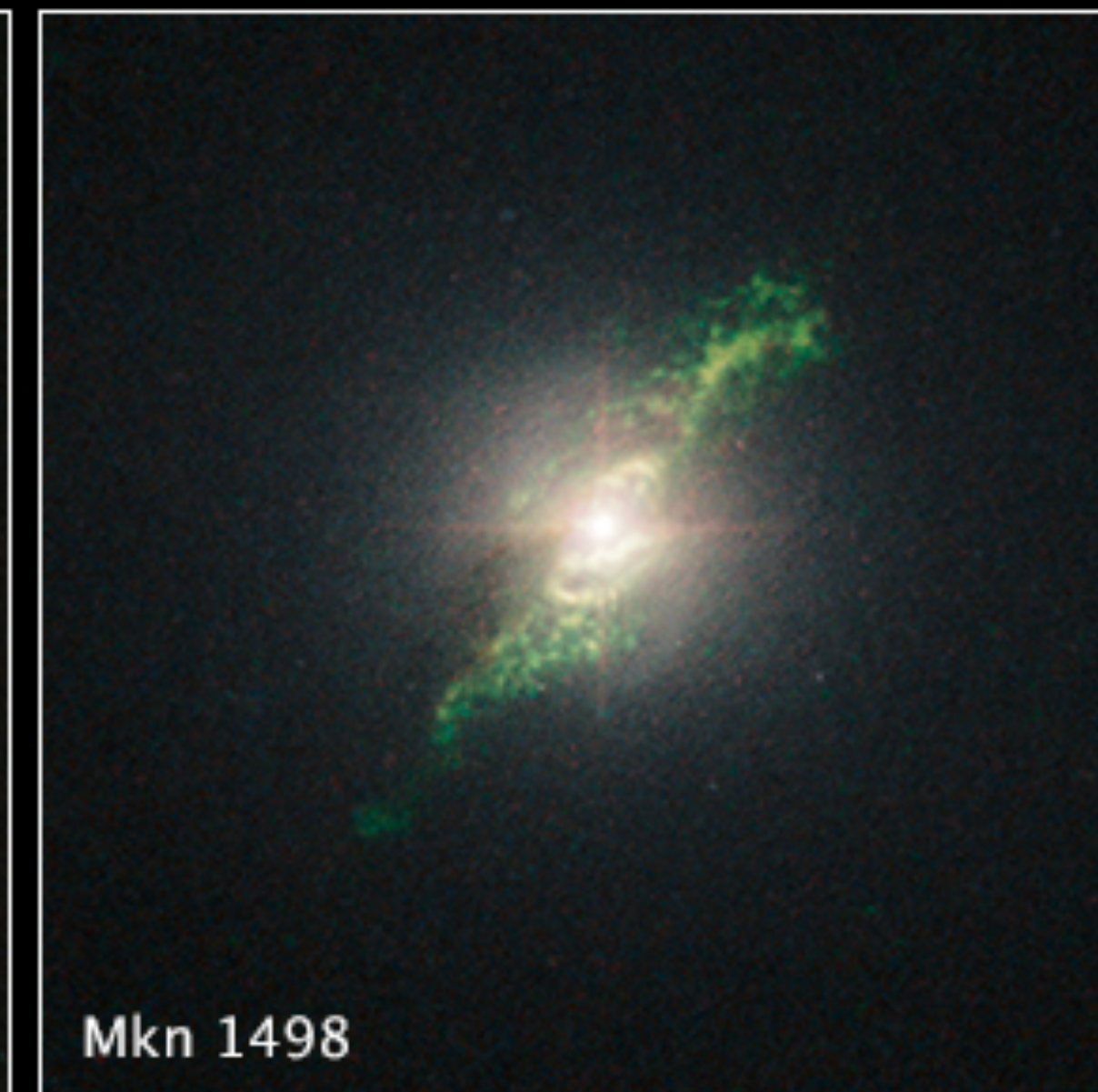
SDSS 1510+07



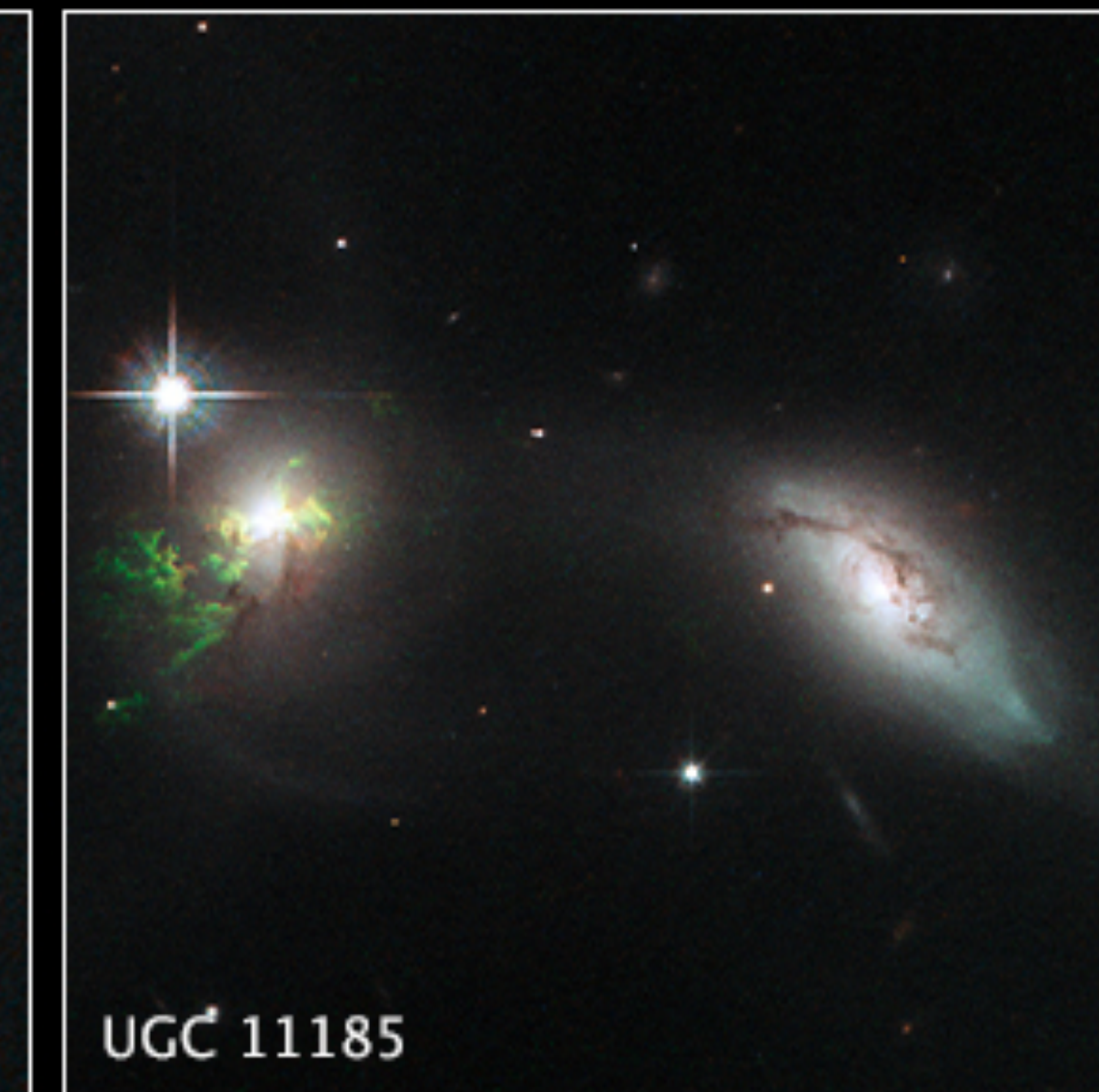
UGC 7342



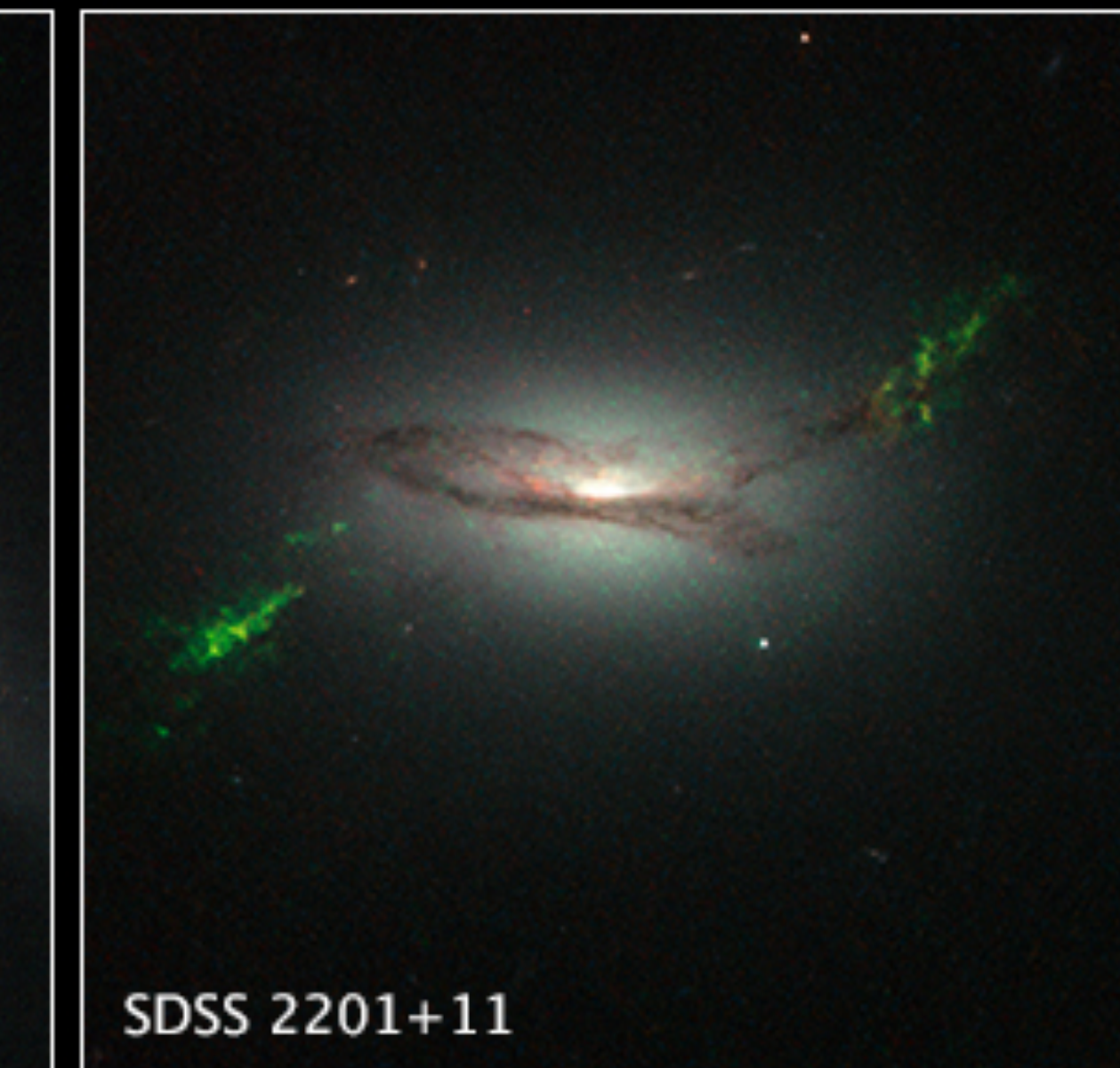
NGC 5252



Mkn 1498

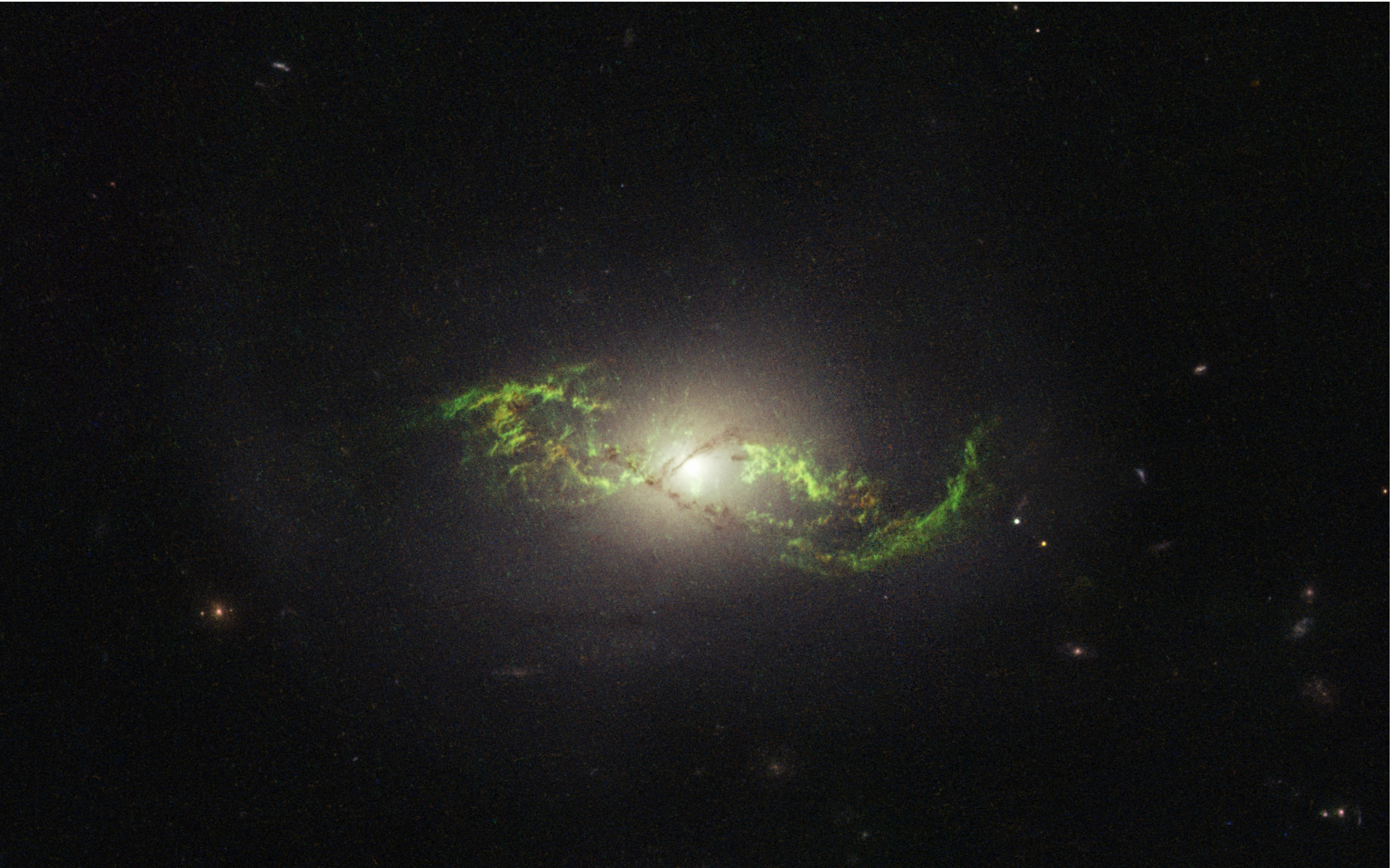


UGC 11185



SDSS 2201+11

# AGN



NGC 5972

AGN, emission  
line nebulas

# AGN

SDSS 2201+11  
AGN, emission  
line nebulas

